



DEPARTMENT OF BIOLOGICAL AND  
ENVIRONMENTAL SCIENCES

# AIR POLLUTION AND DEVELOPMENT OF NORTHERN EUROPEAN SOCIETIES 1966 – 1990

**Kingson Wilson Mattu**

---

Degree project for Master of Science (120 hec) with a major in Atmosphere, Climate and Ecosystems

ES2521, Degree Project Environmental Science HT23

Second cycle

Semester/year: Autumn/Spring 2023/2024

Supervisor: Jan Pettersson

Examiner: Xiangrui Kong

## Abstract

Industrialization has been one of the major influences towards the escalation of atmospheric pollutants after World War II. Metal concentrations in the atmosphere have been increased since the introduction of high-temperature processes such as fossil fuel combustion and smelting. Increased pollutants in the atmosphere have resulted in poor health and increased mortality among individuals, and degradation of the environment. This thesis characterizes aerosol concentration trends in Falsterbo, Southern Sweden, as a function of time from 1966 to 1990 and correlate the results with the meteorological data and air mass back-trajectories, including source apportionment of the elements. The analysis was divided into two parts: initial assessment of 1972 with analysis of filters from each day, and preliminary analysis of 1966 to 1990 with analysis of filters from every eighth day using Energy Dispersive X-ray Fluorescence (EDXRF). Aerosol concentrations in 1972 were analyzed using Hybrid Single-Particle Lagrangian Integrated Trajectory (HYSPLIT) model to generate air mass back trajectories and determine the origin and distance of air masses entering Falsterbo, followed by Positive Matrix Factorization (PMF) analysis to determine the source apportionment of the aerosols. Concentration Weighted Trajectory (CWT) was conducted using openair function in R Studio to illustrate origin of emission. In conclusion, this study found that archived filter samples can be used for characterization of daily changes in aerosol composition in Falsterbo. Long-range air pollutants carried by air masses from Eastern and Southern Europe contribute to the local air quality. Main sources of these aerosols in 1972 were anthropogenic activities such as industrial activities, coal combustion, oil combustion, biomass burning, dust and marine aerosol. Even though various elements were present in every filter of 1972, lead (Pb) and arsenic (As) were not present in all the filters. Lastly, variation in aerosol concentration and their sources of emission can be studied in detail from 1966 to 1990 in 24-hour resolution.

# Table of Contents

Abstract.....	2
List of Figures.....	4
1. Introduction.....	6
2. Background.....	7
3. Methodology.....	12
3.1. Sample Collection and Preparation.....	13
3.2. EDXRF.....	15
3.3. Air mass Back Trajectory Analysis.....	16
3.4. Soot Analysis.....	18
3.5. PMF Analysis.....	20
4. Results and Discussion.....	23
4.1. Initial Assessment of 1972.....	23
4.1.1. Results from Meteorological Data from SMHI.....	23
4.1.2. Results from EDXRF.....	24
4.1.3. Results from PMF Analysis.....	30
4.1.4. Results from Air Mass Trajectory Analysis.....	36
4.2. Preliminary Assessment.....	42
5. Conclusions.....	47
6. References.....	49

# List of Figures

**Figure 2.1:** Production trend of lead (in tonnes) in Gasoline in USA from 1926 to 1989, with the sum of 7 million tonnes of lead burned as leaded gasoline in United States between the mentioned time series (Nriagu, 1990)..... 8

**Figure 2.2:** SO<sub>2</sub> (in µg/m<sup>3</sup>) reduction in Copenhagen since the late 1960s to mid-2000s (Fenger, 2009). ..... 9

**Figure 2.3:** Various sources of lead in Sweden from 1880 to 1980 (Bergbäck et al., 1992). ..... 10

**Figure 2.4:** Location of Falsterbo Lighthouse, Sweden (55.383796°N, 12.816399°E)..... 12

**Figure 3.1:** Falsterbo Lighthouse. .... 13

**Figure 3.2:** Filter selection from archive..... 14

**Figure 3.3:** Filters cut and placed in petri dish..... 14

**Figure 3.4:** (a) Actual filter from 1972, (b) B1 and B2 spots on back side of filter to evaluate blank value. .... 15

**Figure 3.5:** EDXRF Apparatus..... 16

**Figure 3.6:** HYSPLIT interface..... 17

**Figure 3.7:** The Magee Scientific “SootScan<sup>TM</sup>” Model OT-21 Optical Transmissometer. .... 19

**Figure 3.8:** EPA PMF v.5.0 interface. .... 20

**Figure 3.9:** Base model runs in EPA PMF v.5.0. The number of base runs were selected to 20 times..... 21

**Figure 3.10:** Determining factors with Q(true)/Q(robust). .... 22

**Figure 3.11:** (a) Temperature (in °C) of Falsterbo in 1972, (b) wind direction entering Falsterbo in 1972. .... 23

**Figure 3.12:** Time series of elements (in ng/m<sup>3</sup>) characterized by EDXRF from Falsterbo 1972. .... 25

**Figure 3.13:** (top to bottom) S, BC, C, Br, Pb, Si, Ar and Fe concentrations (in ng/m<sup>3</sup>) as a function of time 1972..... 29

**Figure 3.14:** (a) BC and (c) S concentration (in ng/m<sup>3</sup>) correlated with temperature (in °C) as a function of time 1972..... 30

**Figure 3.15:** Solution of factors from 3 to 12. .... 31

<b>Figure 3.16:</b> PMF analysis with Factor 3 to 12, (a) marine s, (b) dusts, (c) combustion/industrialization (d) coal combustion, (e). Oil combustion, (f) combustion/industrialization, (g) industrial, (h) biomass burning.....	35
<b>Figure 3.17:</b> (a) mean clustered air mass back trajectory entering Falsterbo in 1972 (total run time: -72 hr), (b) Element concentrations in each cluster. ....	36
<b>Figure 3.18:</b> CWT technique with element concentration (in ng/m <sup>3</sup> ) and their respective region of Europe.....	38
<b>Figure 3.19:</b> CWT technique with element concentration (in ng/m <sup>3</sup> ) with source factor and their respective region of Europe. ....	40
<b>Figure 3.20:</b> Industries in Czechoslovakia (Kunc et al., 2018).....	41
<b>Figure 3.21:</b> Different types of filters from 1966 to 1990. ....	42
<b>Figure 3.22:</b> Aerosol concentration (in µg//m <sup>3</sup> ) in the function of time 1966 to 1990. ....	44
<b>Figure 3.23:</b> Mean concentration (in µg//m <sup>3</sup> ) per year of S, Cl, Fe, Zn, As, Pb and Si from 1966 to 1990. ....	45
<b>Figure 3.24:</b> BC emissions by energy consumption (in Tg C year <sup>-1</sup> ) per year by country (Hoesly et al., 2018). ....	46

# 1. Introduction

Historically, Industrialization has contributed to the increase of atmospheric pollutants after World War II. This phenomenon has been a concern in Europe since the industrial revolution, particularly in major cities such as London, which have been heavily affected since the past few decades. Metal concentrations in the atmosphere increased since the surge in high-temperature processes such as fossil fuel combustion and smelting (Galloway et al., 1982), and technological development such as fossil fuel combustion processes led to poor air quality in densely populated industrial areas (Brimblecombe, 1999). The health and wellbeing of city dwellers were affected by such phenomenon. Due to rapid economic and population growth in the past decades, and increased and unregulated air pollutant emissions, many premature deaths have occurred and concerns about air quality increased (Murray, 2013).

Increased aerosol concentrations such as sulfate and particulate matter (PM<sub>2.5</sub>) in the atmosphere with long-term exposure have contributed to poor health and increased mortality such as cardiovascular diseases, respiratory diseases, cardiopulmonary and lung cancer mortality, and death among individuals (Barregard et al., 2006; Pope et al., 1995; Zhang et al., 2021). As such, premature deaths in 1952 due to the infamous London smog motivated the ratification of the Clean Air Act of 1956 in United Kingdom (Brimblecombe, 1987). Since then, many legislations upon air quality have been ratified, from local to regional scales, reducing air pollution concentrations in many European countries at the local and national level.

Sweden was also affected by poor air quality due to industrialization. Since the 1970s, various legislations have been ratified to improve the quality of air. Today, local aerosol emissions in Sweden have decreased since the past few decades, however, aerosols carried by air masses from other parts of Europe still affect the atmosphere. Hence, long-range aerosol transport is still a major contributor to air pollution. One study from (Olstrup et al., 2018) states that long-range transport and local emissions both are the main sources of air pollutants in Sweden. Although efforts with improving air quality on national scale are being effective to mitigate the aerosol concentration level in Sweden, long-range pollutant influx from other parts of the Europe should also be considered. Air quality legislations require to be on the regional scale in order to improve the air quality of Sweden even further.

This thesis studies the aerosol concentration trends of Falsterbo, Sweden, as a function of time from 1966 to 1990. Additionally, air mass back-trajectories in Falsterbo have been considered for the year of 1972, followed by source apportionment, to understand the transboundary transport of aerosols entering Southern Sweden and determine their emission sources respectively. Finally, this paper also recommends future recommendations of variation in aerosol concentration and their sources of emission can be studied in detail from 1966 to 1990 in 24-hour resolution.

## 2. Background

Air pollution has been a major factor in the damage to the environment and human health since the industrial revolution. Population growth and advance in technology increased use of fossil fuels. Combustion engines came into use as socio-economic development increased. This was seen as symbol of growth and prosperity for the society after the World War II (Fenger, 2009). The postwar world was more focused on development and prosperity that led to increased industrial activities and higher coal emissions (Brimblecombe, 2006).

The Great Smog of 1952 in London, caused by high sulfur dioxide and soot emissions, was the cause of thousands of deaths and the beginning of the Clean Air Act of 1956, which aimed to reduce air pollution and improve air quality in the UK (Brimblecombe, 2006; Fenger, 2009; Koolen & Rothenberg, 2019). Since then, air quality became a major concern in many countries and many initiatives had been taken to control air pollution as mortality rose. For example, 5-day smog was reported in parts of West Germany in 1985 that increased mortality and morbidity in the polluted area (Wichmann et al., 1989).

As transport became popular, lead emissions from vehicle fuel came under highlight. It was considered environmentally unsafe. Organolead compounds were used as antiknock agents to gasoline for vehicle and about 90% of gasoline in United States was lead-based during 1960s. This led to consumption of 375,000 tons of lead in the year of 1970 worldwide (Grandjean & Nielsen, 1979; Nriagu, 1990).

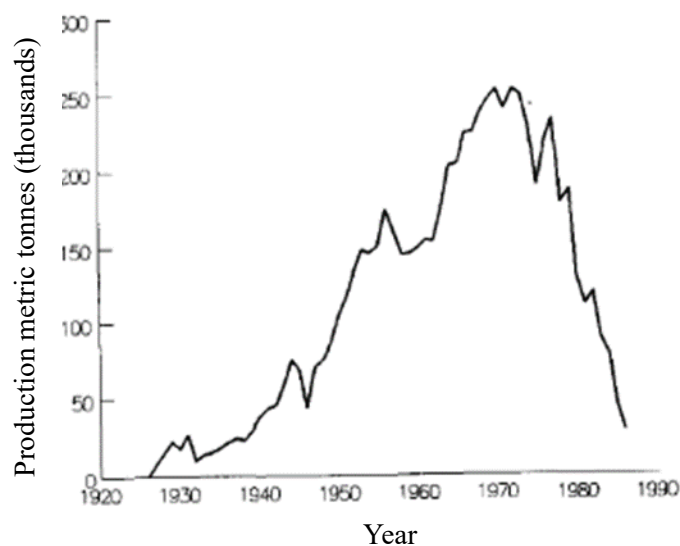


**Figure 2.1:** Production trend of lead (in tonnes) in Gasoline in USA from 1926 to 1989, with the sum of 7 million tonnes of lead burned as leaded gasoline in United States between the mentioned time series (Nriagu, 1990).

Consumption of leaded gasoline in the United States is illustrated in Figure 2.1. Consumption rate increased steadily since the 1930s with the highest peak in 1970s, showing the popularity of the leaded gasoline in the United States. After awareness to significant public health concerns, the Clean Air Act of 1970 in the US initiated a ban on leaded gasoline, which significantly reduced atmospheric lead concentrations (Nriagu, 1990; Schmalensee & Stavins, 2019). Legislations to improve air quality, such as the Clean Air Act of 1956 in the UK and the Clean Air Act of 1970 in the US, have been implemented to mitigate air pollution and reduce lead and sulfur dioxide emissions (Brimblecombe, 1987; Nriagu, 1990).

Various legislations in different countries of Europe have been applied to reduce various aerosols and urban air quality has been regulated by air quality standards (Fenger, 2009). For example, Figure 2.2 shows the reduction of sulfur dioxide in Copenhagen's atmosphere. The highest yearly average peak was observed in the late 1960s with more than  $80 \mu\text{g}/\text{m}^3$ . The concentration starts to decrease from 1970s and further reduces below  $20 \mu\text{g}/\text{m}^3$  in mid 2000s. Due to increased monitoring stations and various legislations being implemented, reduction of  $\text{SO}_2$  was successfully achieved in Copenhagen (Fenger, 2009).

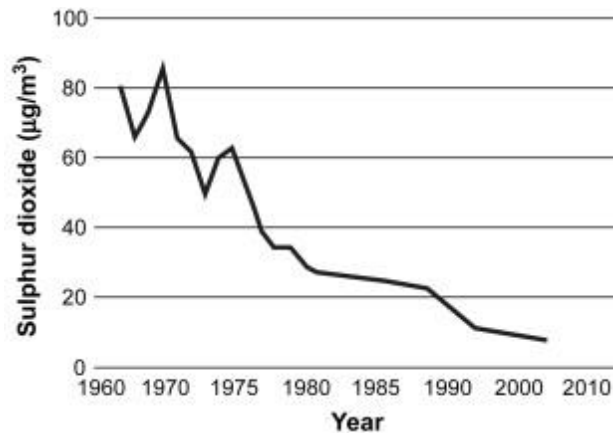


*Figure 2.2: SO<sub>2</sub> (in µg/m<sup>3</sup>) reduction in Copenhagen since the late 1960s to mid-2000s (Fenger, 2009).*

Many European countries have mitigated lead emissions and regulated aerosol concentrations in the atmosphere. These regulations were used to gradually decrease the level of long-term exposure to particulate matter and this process took few years to reduce air pollutants (Anderson, 2009; WHO, 1979, 2006). However, many developing countries have not established regulations that are required to mitigate aerosol concentrations on a regional scale, and unwanted air pollution can be observed despite air quality legislations are being implemented in Europe (Fenger, 2009; Nriagu, 1990). It is important to note that even if some countries managed to reduce the amount of aerosol emissions from their atmosphere, other countries that are still dependent on energy from combustion plants and engines which results in the contribution to the aerosol emissions in other countries. Furthermore, many European countries have managed to reduce emissions, however, emissions from non-European countries needs to be regulated also in order to mitigate PM<sub>10</sub> emissions entering European atmosphere (Yang et al., 2020). Air pollution and mortality is still a major concern. In 2015, PM<sub>2.5</sub> was ranked fifth in mortality risk factor (Cohen et al., 2017). Additionally, long-range pollutants are expected to travel from continent to continent.

During the 19<sup>th</sup> century, Sweden had various sources of energy supply such as wood, charcoal and hydropower. But coal imports grew due to rapid industrialization after 1870 (Kaijser & Högselius, 2019). Later in the 1920s, Sweden experienced rapid economic growth, especially by increased car manufacturing and oil imports (Kaijser & Högselius, 2019). Hence, Sweden was heavily dependent on coal imports before World War II and postwar. Later in 1952, it was the first country to build a 400-kV hydropower transmission line. Coal was replaced with heavy oil in industrial

applications and urban areas in the late 1940s and the share of coal reduced to approximately 40% in 1950.

Tetraethyl lead was introduced in gasoline production as an antiknock agent after World War II in Sweden, and lead emissions were at its peak during 1970, making automobile usage the major source of lead emission to the atmosphere and soil, including consumption emissions such as leads used in paints, lead oxides, cables and batteries (Bergbäck et al., 1992). Figure 2.3 illustrates the relative share of lead emission source per decade from 1880 to 1980 in Sweden.

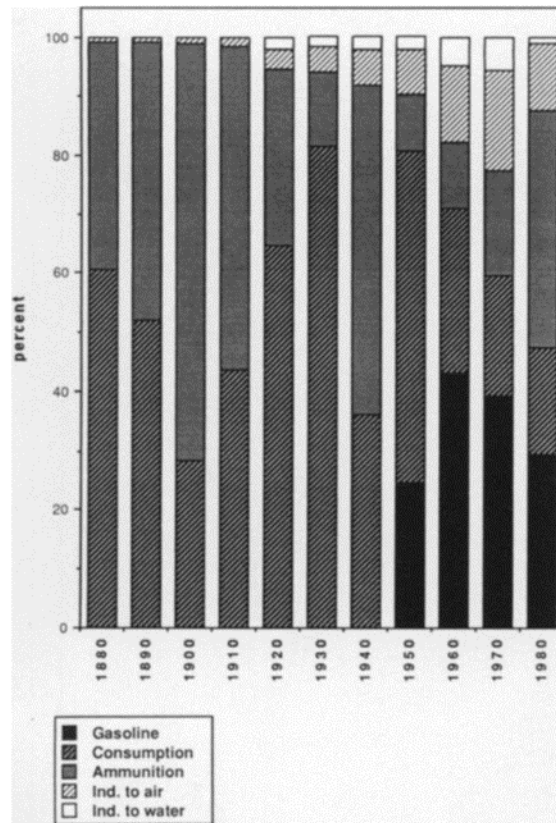


*Figure 2.3: Various sources of lead in Sweden from 1880 to 1980 (Bergbäck et al., 1992).*

Leaded gasoline started to become popular in the 1950s and increased during the 1960s (in Figure 2.3). The share trend for leaded gasoline started to fall from 1970s and onwards. Since the 1970s, developed countries, including Sweden, started regulating lead and various aerosols from vehicles emissions by banning lead as antiknock agent, and the approaches were successful to reduce the lead and heavy metal concentrations from the atmosphere (Guerreiro et al., 2014; Murray, 2013). However, these aerosols were not eliminated completely. There were other sources of heavy metals that still exist in the troposphere of Sweden excluding emissions from vehicle combustion engine.

Few examples of sources are brake linings in vehicles that contribute to Cu, Pb and Zn emissions, tires of vehicles contributing to Zn, Pb, Cr, and Ni, asphalt wear contributing to Cu, Zn, Ni, Pb and Cr, and coal combustion contributing to As, Pb, S and black carbon (Sörme et al., 2001; Wang et al., 2016). It has been mentioned in a 2014 report that effective policies for reduction of air pollution still remains a challenge (Guerreiro et al., 2014).

In another study it was found that heavy metal concentrations were high among mosses in rural areas of Sweden where industrial emissions were minimum, suggesting that long-range transport appears to contribute to heavy metal aerosol concentrations in the atmosphere that were deposited on the mosses (Harmens et al., 2004). Furthermore, Southern Scandinavia is likely the most exposed region to long-range aerosol pollution from industrial centers in Central Europe and England, due to south-westerly winds (Hovmand & Kystol, 2013). Interestingly, long-range transport was observed centuries ago. For example, the first long-range pollutant was recorded in the fifteenth century, where the pollutants from biomass burning in Scotland damaged the vine crops in France. It was also expected that pollutants from the British Isles could travel to Scandinavia via westerly winds (Brimblecombe, 1987).

The Swedish Meteorological and Hydrological Institute (SMHI), with the permission of the Swedish National Administration of Shipping and Navigation, and Air Protection Division of the Swedish National Environmental Protection Board (Brosset & Åkerström, 1972), initiated a project of measuring daily mean values of air-borne particulate matter (soot) and particle-borne sulfur during the 1960s. Initially, six stations were established in Sweden in the beginning of the project, and the Falsterbo lighthouse (55.383796°N, 12.816399°E) was one of the six stations with the longest time series from 1966 to 2020. Lighthouse stations were used specifically to measure background long-range transport of black carbon, as they are not located in hotspot areas such as the major cities. The sampling probe to capture the black carbon was placed at the tower of the lighthouse (Brosset & Åkerström, 1972).

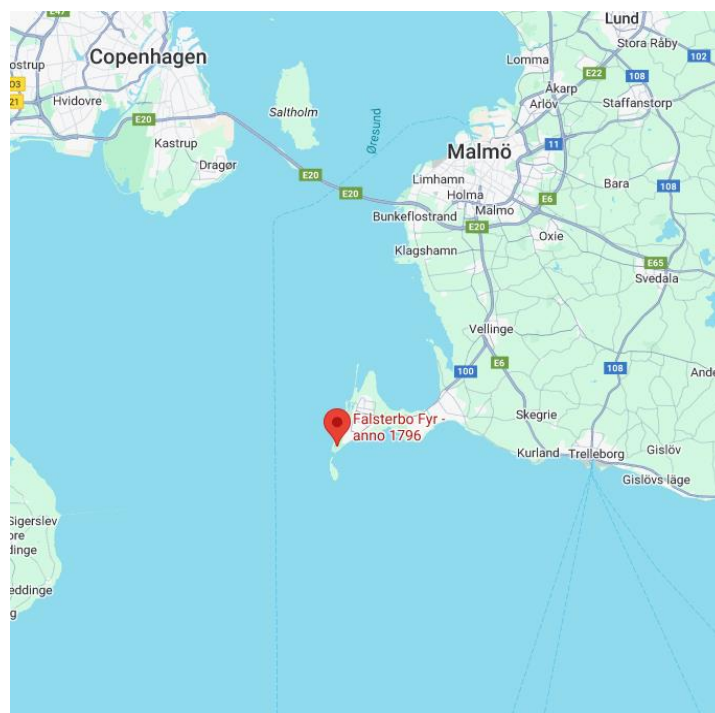


*Figure 2.4: Location of Falsterbo Lighthouse, Sweden (55.383796°N, 12.816399°E).*

Recently, IVL Svenska Miljöinstitutet AB research institute, a subsidiary of the Foundation Institute for Water and Air Pollution Research (SIVL), collaborated with SMHI and gained access to the archived filters from Falsterbo lighthouse, and provided the filters to University of Gothenburg to study and analyze the filters in detail.

### 3. Methodology

In this project to characterize the variation of aerosols and their respective concentration in the air as a function of time, the sampling probe was placed 24 meters above ground level (AGL) at the tower of Falsterbo lighthouse (Brosset & Åkerström, 1972), and a filter was placed inside the probe. A specific volume (in liters) of air was passed through the filter, trapping aerosols within it. Each filter's sampling time was approximately 24 hours before being replaced with a new filter the next day. The volume of air and time the filter was placed and removed were noted on the filter. The project, running from March 1966 to December 2020, collected and stored approximately 20,000 filters in total.



*Figure 3.1: Falsterbo Lighthouse.*

To conduct this thesis, the archived filters from Falsterbo lighthouse were collected from IVL. The project was divided into two parts: initial assessment with filters of 1972 to understand if the filters contain any aerosol concentrations, followed by preliminary assessment to characterize the concentration of aerosols from 1966 to 1990. Quantitative elemental analysis was conducted by using Energy Dispersive X-Ray Fluorescence (EDXRF), followed by soot analysis. The results were then subtracted with a blank filter to remove any background signals from the data. Furthermore, Air mass back-trajectory analysis was conducted to observe the long-range aerosols carried by the air mass patterns around the southern region of Sweden. Finally, source apportionment was carried out by Positive Matrix Factorization (PMF) analysis to correlate the element concentrations in the samples and determine the source of emissions.

### 3.1. Sample Collection and Preparation

Experimental procedure began with the collection of 365 filters from 1972. One filter was missing. The filters are Whatman No.1 filters (Brosset & Åkerström, 1972). This produced the initial assessment. Subsequently, filters from 1966 to 1990 were collected at 8-day intervals to reduce the sample size. Thus, sample size was reduced from 20,524 to 1103 samples. However, some filters were missing, so the closest available dates were used as replacement.

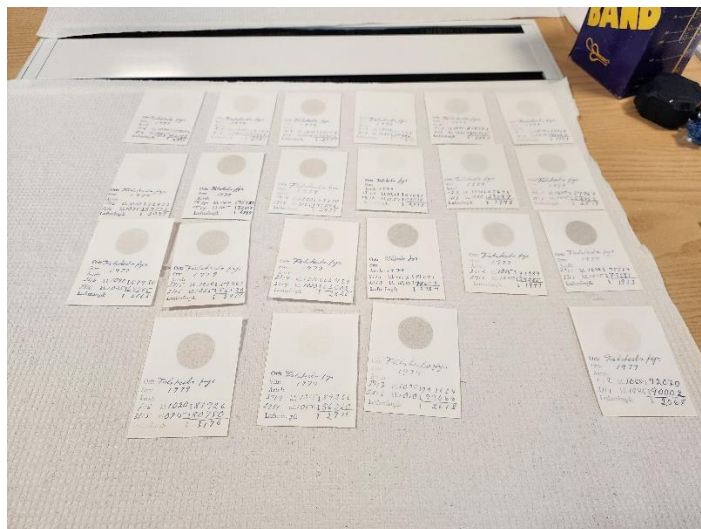


*Figure 3.2: Filter selection from archive.*

Figure 3.2 shows the Whatman No. 1 filters that were collected from Falsterbo lighthouse. The samples, rectangular filters with a height of 8.7 cm and width of 6.6 cm, were cut into circular shapes with a diameter of 3.95 cm with a cutting tool to fit into the sample tray. The cuts were made carefully to keep the spot at the center of the filter. The samples were then placed in petri dishes (see Figure 3.3) and sealed to prevent contamination. No other treatment was required for the filters and the method was non-destructive.



*Figure 3.3: Filters cut and placed in petri dish.*

There were no blank filters in the filter archive from 1966 to 1990 except for two unused blank filters that were found in 1971 and 1976 archive. These two filters, however, had contaminations

of few elements. To find a blank value for the rest of the elements that were present in the unused filters, various parts of filters outside the soot spot (see Figure 3.4) were analyzed by EDXRF.

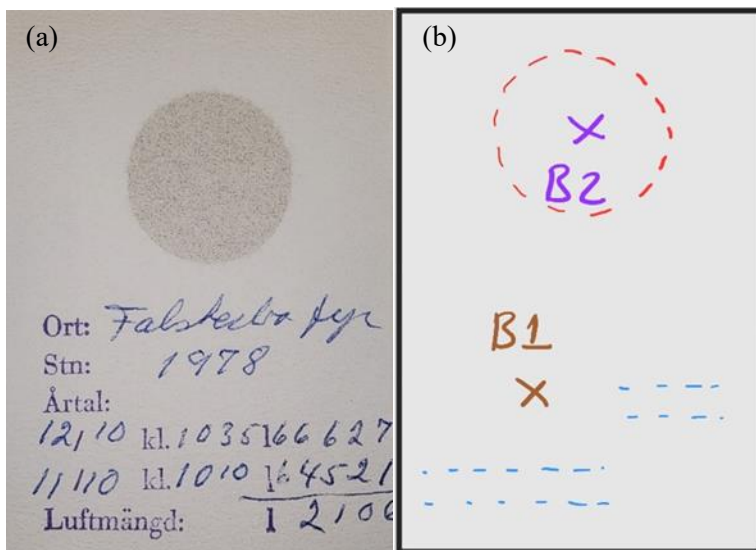


*Figure 3.4: (a) Actual filter from 1972, (b) B1 and B2 spots on back side of filter to evaluate blank value.*

Two different spots were considered to evaluate blank values. Figure 3.4 shows the filter and an illustration of two different areas that were analyzed to determine a blank value. B2 spot was the opposite side of the soot spot and B1 was behind the filter and outside the soot spot. B1 was useful to find the minimum values of the elements to be used as a blank, except for Cu and Zn contamination. This contamination was likely due to the brass plates in the sampling probe that was used to hold the filter while the volume of air was passed through. To find minimum values for the rest of the elements that were not found in the blank or in B1 and B2 area, an average of five lowest values observed were used instead to determine the background levels. The lowest values were determined from combination of measurements of the soot spot and different areas of the backside of the filters.

### 3.2. EDXRF

Energy Dispersive X-ray Fluorescence (EDXRF) spectrometer (see Figure 3.5) was used to analyze the collected filters. The apparatus projects an x-ray beam into the filter to ionize the aerosol particles under the detection limit (DL). The atom of the particle releases an electron from its inner shell, and electron from outer shell drops into the gap of the inner shell. This movement of electron emits fluorescence radiation. As such, an element can be identified by its characteristic

fluorescence radiation. A semiconductor detector then collects the emitted fluorescence radiation, and the energies are sorted and processed in a multichannel analyzer. The produced spectrum can be obtained on the monitor that shows the photon energy on the x-axis and number of photons counted on the y-axis.

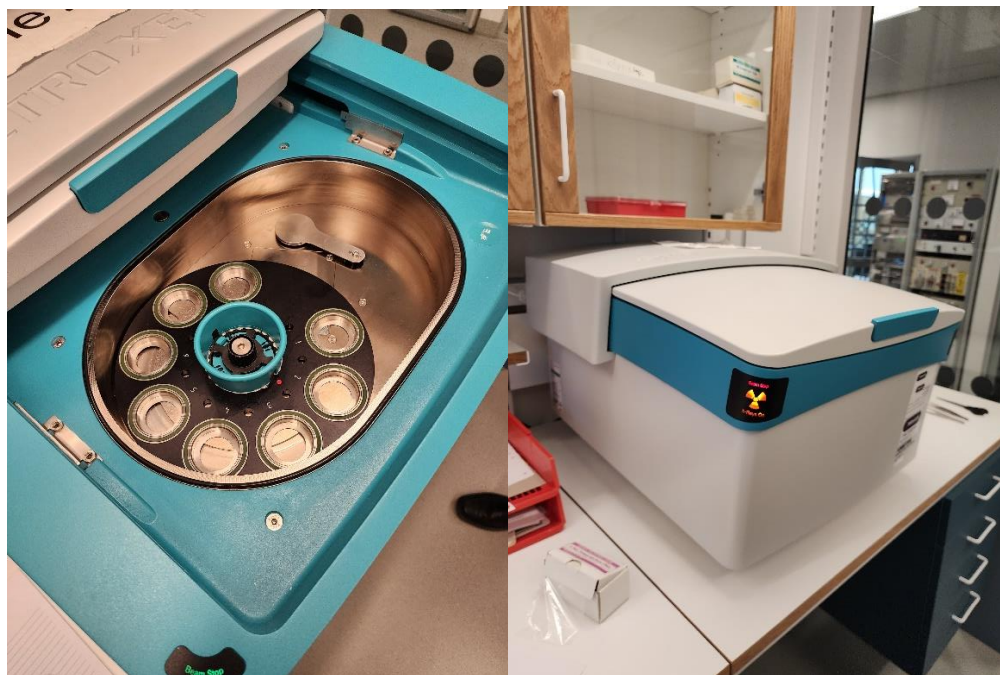


*Figure 3.5: EDXRF Apparatus.*

The spectrometer used a chromium X-ray tube and palladium (Pd) and cobalt (Co) anodes with the voltage adjusted to 40 kV and current adjusted to 1.0 mA (Kovacevik et al., 2011). A total of 8 filters were placed in the sample changer at a time, that automatically changed the filter after analysis was completed. Each analysis run with 8 samples took approximately 3 hours to complete, and per filter took approximately 23 minutes to complete.

### 3.3. Air mass Back Trajectory Analysis

Hybrid Single-Particle Lagrangian Integrated Trajectory Model (HYSPLIT) is a resourceful atmospheric transport and dispersion model that is capable to compute air parcel trajectories in a given time, including complex transport, deposition and chemical transformation simulations (Draxler & Hess, 1998). Created by National Oceanic and Atmospheric Administration (NOAA), the model was used back in 1949 when Special Project Section (SPS) of US Weather Bureau tried to track radioactive debris in the air mass during the first Soviet atomic test (Stein et al., 2015).

Today, HYSPLIT is commonly used for back-trajectory and cluster analysis to trace the origin of air masses entering the receptor site (Fleming et al., 2012).

For this study, each trajectory was set to 72 hours in a backward direction. To collect the back trajectory for 1<sup>st</sup> January 1972, the starting date in trajectory setup was 27<sup>th</sup> December 1971 to collect the trajectories for the last 3 days of December.

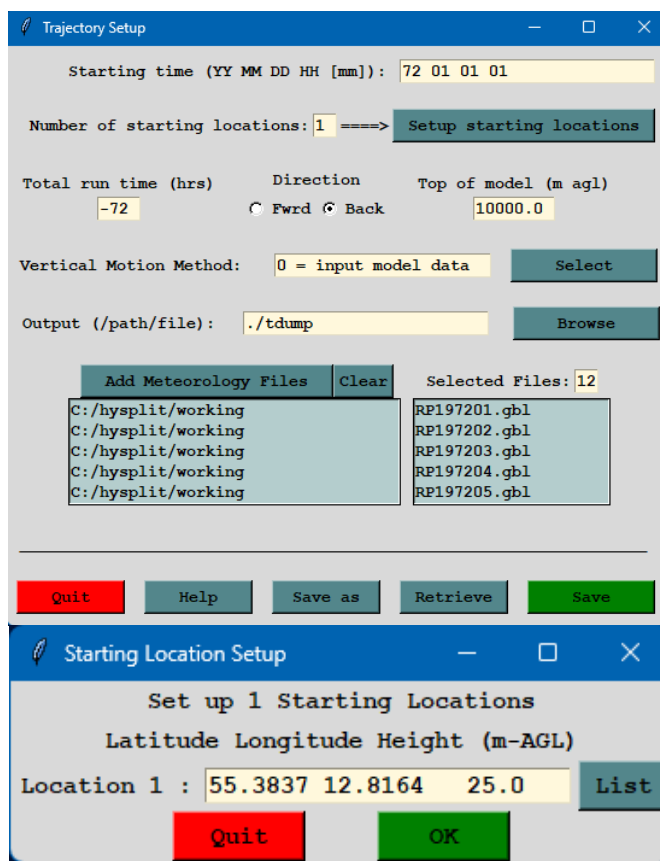


Figure 3.6: HYSPLIT interface.

Cluster analysis grouped similar back trajectories to simplify descriptions and determine atmospheric transport patterns (Fleming et al., 2012). These groups of similar trajectories are called clusters, and they represent the mean trajectory of a specific atmospheric transport flow. Furthermore, this tool groups the trajectories by distance and direction of the air mass in a given time (Stunder, 1996). Furthermore, by combining EDXRF analysis to evaluate air pollutant concentrations with the back trajectory cluster analysis, it is possible to determine detailed information of long-range air pollutants and the region from where the air mass came from to the receptor site (Karaca & Camci, 2010). Such approach allows to analyze significant differences in

concentration of atmospheric pollutants with the air mass cluster, and hence, determines the origin of the pollutants (Baker, 2010).

HYSPLIT analysis for long-range transport was performed for 366 days in 1972 using HYSPLIT software v.5.3.0. As NOAA has been storing meteorological data since 1949 globally, it was possible to acquire back trajectories of Falsterbo from 1972 from the meteorological database. Archived data from each month of 1972 was downloaded from the NOAA servers and the setup was run with the coordinate receptor site 55.3837, 12.8164 and each trajectory's total run time of -72 hours with 2-hour interval between trajectories. Hence, each trajectory was projected backwards for a 3-day period from the receptor site (see Figure 3.6), with 12 trajectory projections per day. AGL was selected to 25 m due to the height of the lighthouse where the sampling probe was placed. AGL plays an important role in the HYSPLIT analysis; increasing AGL decreases short-slow-moving air mass and increases long-fast-moving air mass (Markou & Kassomenos, 2010). For this reason, AGL from receptor site was selected according to the height of the tower of lighthouse, and top of model AGL was set to 10,000 m. This ensured that trajectories included short-slow-moving air mass around Falsterbo and long-range air mass from other parts of Europe.

### 3.4. Soot Analysis

The Magee Scientific "SootScan<sup>TM</sup>" Model OT-21 Optical Transmissometer (Figure 3.7) was used to analyze black carbon (BC) of the filters. The apparatus analyzes filter composition for black carbon and brown carbon, calculating the absorbance data at two different wavelengths: ultraviolet (370 nm) and infrared (880 nm) wavelengths. It consists of a filter tray with two slots, one called "position 1" to hold the sample filter and another called "position 2" to hold a blank filter. This allows for accurate transmission measurements.



**Figure 3.7:** The Magee Scientific “SootScan™” Model OT-21 Optical Transmissometer.

Initially, the apparatus scans the blank filter to determine the background signals, then the rest of the analysis can be made with the same blank measurements. Sample attenuation can be measured against an unexposed filter in the apparatus for more accurate measurements (Sreekanth et al., 2019). Then the apparatus calculates attenuation by the following formula (*in correspondence to Beer-Lambert Law:  $A = \epsilon bc$* ):

$$\text{Attenuation} = 100 * \ln \left( \frac{\text{blank filter transmitted intensity}}{\text{sample filter transmitted intensity}} \right)$$

Furthermore, the apparatus calculates UV and IR attenuations separately according to the following formula:

$$\text{Attenuation} = 100 * \ln \left( \frac{\text{UVB}}{\text{UV}} \right)$$

and

$$\text{Attenuation} = 100 * \ln \left( \frac{\text{IRB}}{\text{IR}} \right)$$

UVB: Ultraviolet Blank Filter transmitted Intensity

UV: Ultraviolet Sample Filter transmitted intensity

IRB: Infrared Blank Filter transmitted intensity

IR: Infrared Sample Filter transmitted intensity

These calculations are then recorded in the software that is connected to a computer using USB type-B port.

IR attenuation is used to analyze black carbon while UV attenuation is used to analyze brown carbon. However, only IR attenuation was considered for this study. UV attenuations were excluded because brown carbon is an organic material, can be volatile and decompose, and measurements were affected by discoloration of the archived filters. This brought lower confidence towards the brown carbon data as the filters were stacked and stored for several years, which has affected the concentration of organic compounds. The analytical procedure was simple, quick and non-destructive to the filter samples.

### 3.5. PMF Analysis

Positive Matrix Factorization is a multi-variate factor analysis tool that breaks down a matrix of sample data into two different matrices: factor contributions and factor profiles. Users can then interpret the factors and identify the source type of the aerosols on the sample. In this research, PMF was used to determine the sources of aerosol concentrations on the filter from 1972 by analyzing the factors from PMF. Factors were cross-checked with literature to identify emission sources. EPA PMF v.5.0 (see Figure 3.8) was used throughout the analysis.

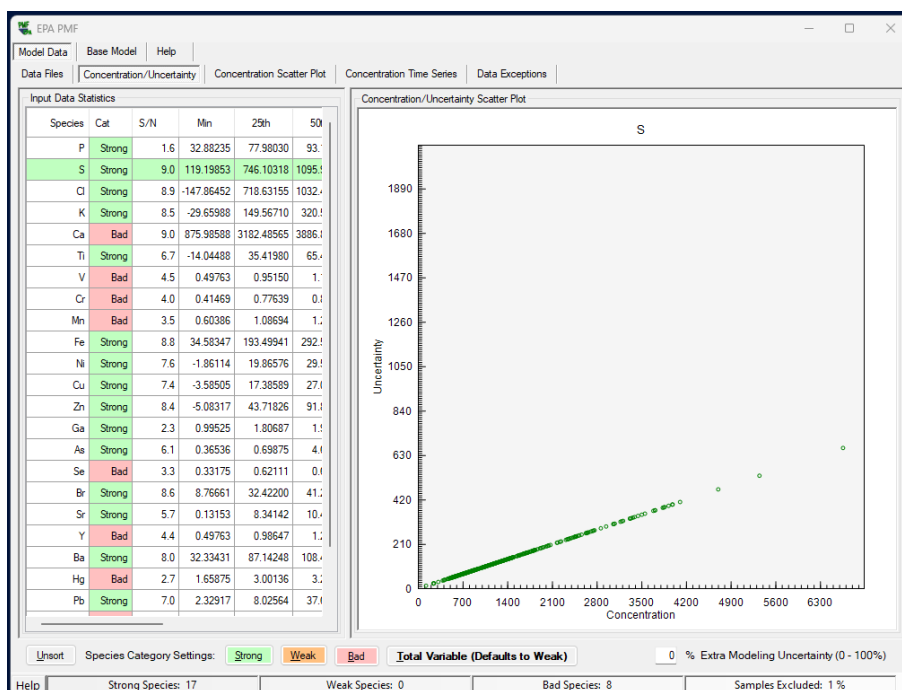


Figure 3.8: EPA PMF v.5.0 interface.

A few elements had to be removed in this analysis. Bi, Hg, Cr and Ca were removed from the analysis as only a few data points were above the detection limit. Furthermore, high concentrations

of Cl and K were observed on 12<sup>th</sup> of February 1972, and it was removed to reduce uncertainties of correlation of the elements and factors. The initial execution of the base model produces the principal probability mass function output, which includes profiles and contributions. Enabling the "Random Start" option initiates the base model run with a fresh random seed or beginning point for iterations. to determine if the found solution is a local or global minimum, it is possible to utilize various random seeds. This will enable users to confirm the consistency of the Q(robust) values. Disabling the "Random Start" option allows for the establishment of a consistent seed. Using the same fixed seed, together with an equal number of factors and runs, will produce consistent PMF results. This seed is also saved in the configuration file. The configuration file may be reloaded later to further evaluate PMF solutions and can be shared with partners for their consideration. In this case, Factors were run with 20 base runs from factor number 3 to 12. Figure 3.9 shows the total number of base runs that were performed in PMF user interface.

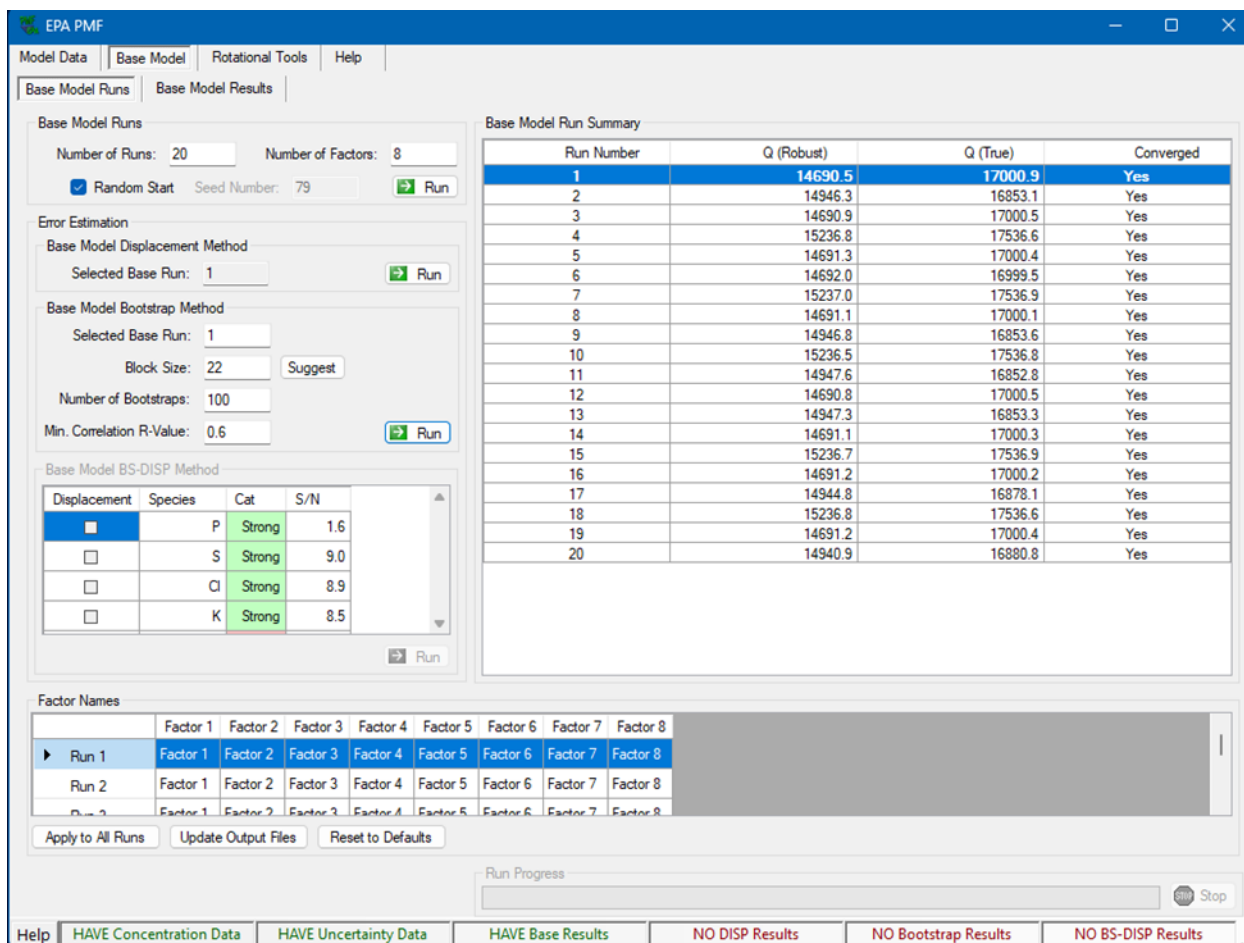
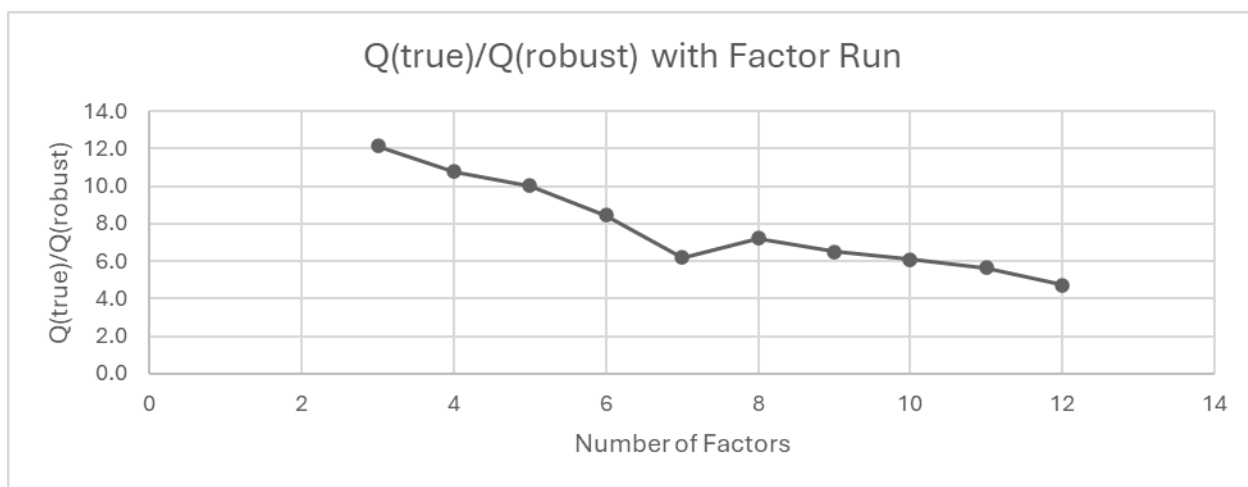


Figure 3.9: Base model runs in EPA PMF v.5.0. The number of base runs were selected to 20 times.

The parameter  $Q(\text{true})$  is a measure of how well the data points match the model, derived using all available data. On the other hand,  $Q(\text{robust})$  is a parameter that measures the degree of fit of a model by removing data points that are not accurately represented. The difference between  $Q(\text{true})$  and  $Q(\text{robust})$  demonstrates the influence of data points with large, scaled residuals. These locations may represent the highest levels of effect from sources that are not constantly present across the whole sample period. Moreover, when the uncertainties are extremely elevated, the values of  $Q(\text{true})$  and  $Q(\text{robust})$  will be comparable, as the residuals are adjusted based on the degree of uncertainty.

$Q(\text{robust})$  is unaffected by data points that are poorly suited by the PMF, making it a vital parameter for picking the ideal run from several iterations. The variability of the robust  $Q$  also reveals the extent to which the outcomes of the initial base run are affected by the random seed used to start the gradient algorithm. If the data exhibits a consistent trajectory towards the minimum, the  $Q(\text{robust})$  values will demonstrate minimal variability across several runs. In contrast, if the initial conditions and the data-defined parameters impact the trajectory towards the minimum, the  $Q(\text{robust})$  values will exhibit variation. In such instances, the  $Q(\text{robust})$  value with the lowest value is usually selected, since it signifies the most ideal option. Nevertheless, it is crucial to acknowledge that little fluctuations in  $Q$ -values do not automatically indicate minimal diversity in source compositions over many iterations.



*Figure 3.10: Determining factors with  $Q(\text{true})/Q(\text{robust})$ .*

Each time  $Q(\text{true})$  and  $Q(\text{robust})$  were noted down in every run to see the impact of data points with high scale residuals. Similar  $Q(\text{true})$  and  $Q(\text{robust})$  results means the uncertainties were high.

This helped to determine how many factors runs were required. Hence, factors 3 to 12 were studied for this project (see Figure 3.10). Factor 10 was then selected as a good representation of the data.

## 4. Results and Discussion

### 4.1. Initial Assessment of 1972

The initial assessment was carried out at the beginning of this project. The results were obtained by EDXRF and analyzed by using PMF analysis for source apportionment, followed by HYSPLIT model for back trajectories, and finally CWT techniques to plot concentrated back trajectories.

#### 4.1.1. Results from Meteorological Data from SMHI

Meteorological data for Falsterbo during 1972 were collected from SMHI database archive. Temperature and wind direction were obtained and used in this study to observe the meteorological situation of the region.

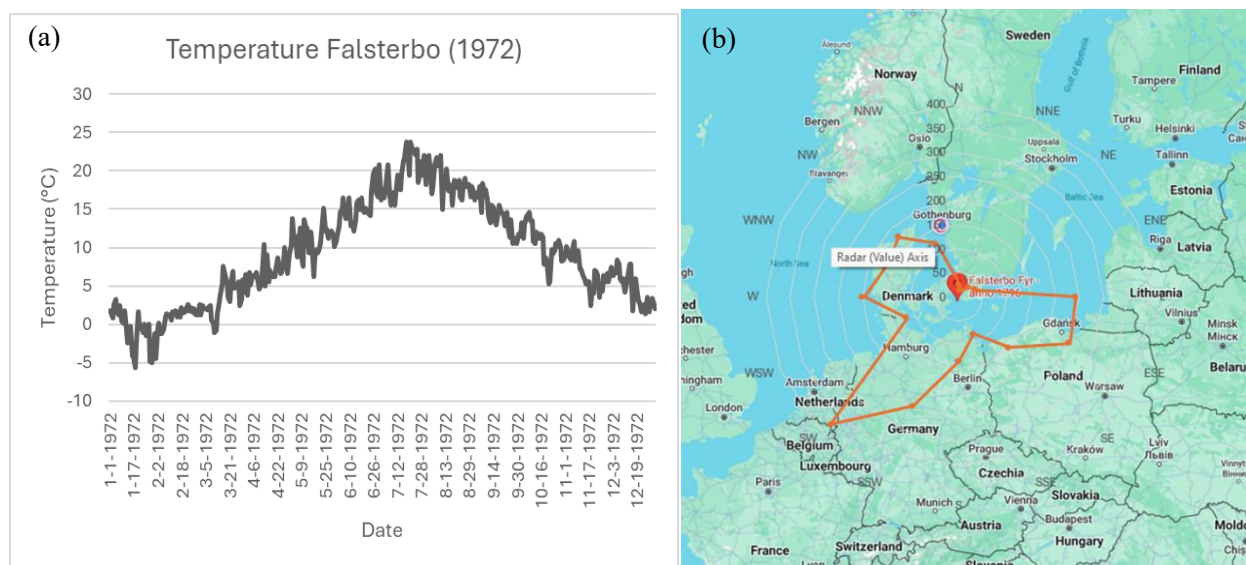


**Figure 3.11:** (a) Temperature (in °C) of Falsterbo in 1972, (b) wind direction entering Falsterbo in 1972.

From Figure 4.1, the highest temperature recorded in 1972 was 23.8 °C during the month of July and the lowest temperature recorded was -5.6 °C during late January. This data was later compared with S and BC (see Figure 4.4) to understand the local source emissions. The wind entering Falsterbo was mostly from Eastern and Southern Europe. Nevertheless, a more detailed analysis of air mass back trajectories in 1972 was conducted later in this study to analyze the wind patterns in detail.

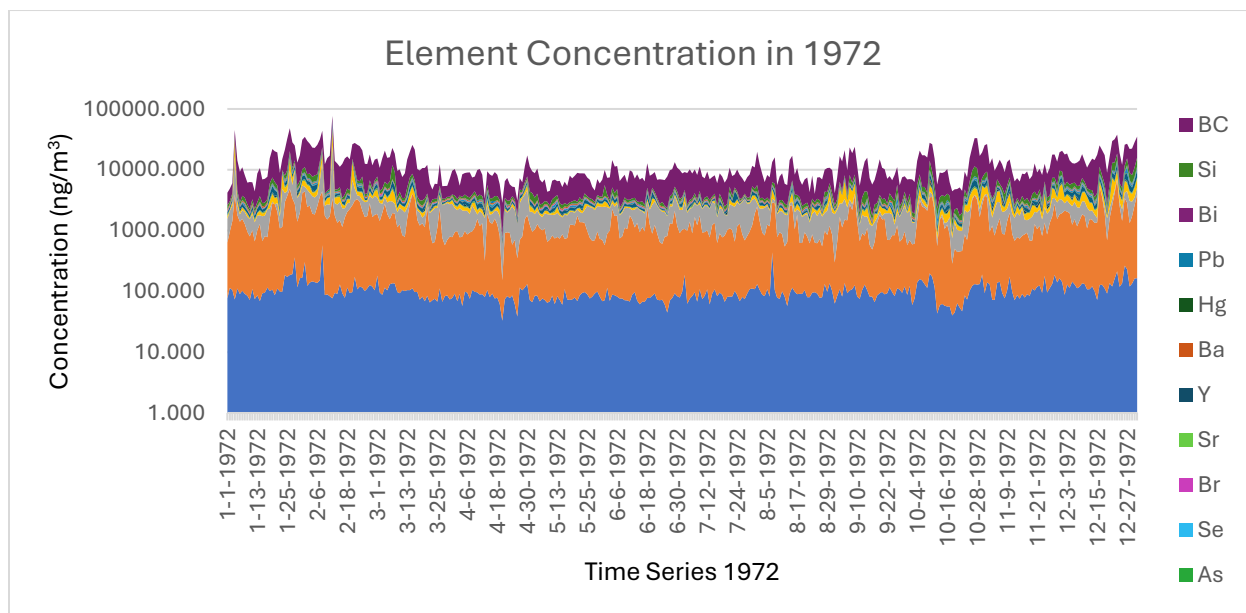
#### 4.1.2. Results from EDXRF

Elements that were over detection limit (DL) in the EDXRF analysis were P, S, Cl, K, Ca, Ti, V, Cr, Mn, Fe, Ni, Cu, Zn, Ga, As, Se, Br, Sr, Y, Ba, Hg, Pb, Bi and Si (see Figure 4.2). Despite determining the blanks, another concern was the air volume measurements that were passed through the filter in the apparatus in Falsterbo. An air pump meter malfunction was noticed during one period. It was initially thought that the air pump had a malfunction. However, aerosol concentrations were relatively high throughout the year of 1972 if compared to filters that contained proper air volume. Hence, it was confirmed that the air pump was not a problem, but the air pump meter had faulty readings. It was later observed that the volume count had a difference in a factor of 10, probably an error while reading and noting down the pump. Hence, volume count of each filter was used for calculating concentration of each day in 1972. EDXRF analysis calculated the concentrations in  $\text{ng}/\text{cm}^2$ . Area of the spot was measured in  $\text{cm}^2$  and the air volume was measured in L and converted to  $\text{m}^3$ . The aerosol concentrations were then converted to  $\text{ng}/\text{m}^3$ .

*Table 3.1: DLs, mean, standard deviation, minimum and maximum concentrations of 1972 (in  $\text{ng}/\text{m}^3$ ). N = number of filters with signals in EDXRF for specific aerosol.*

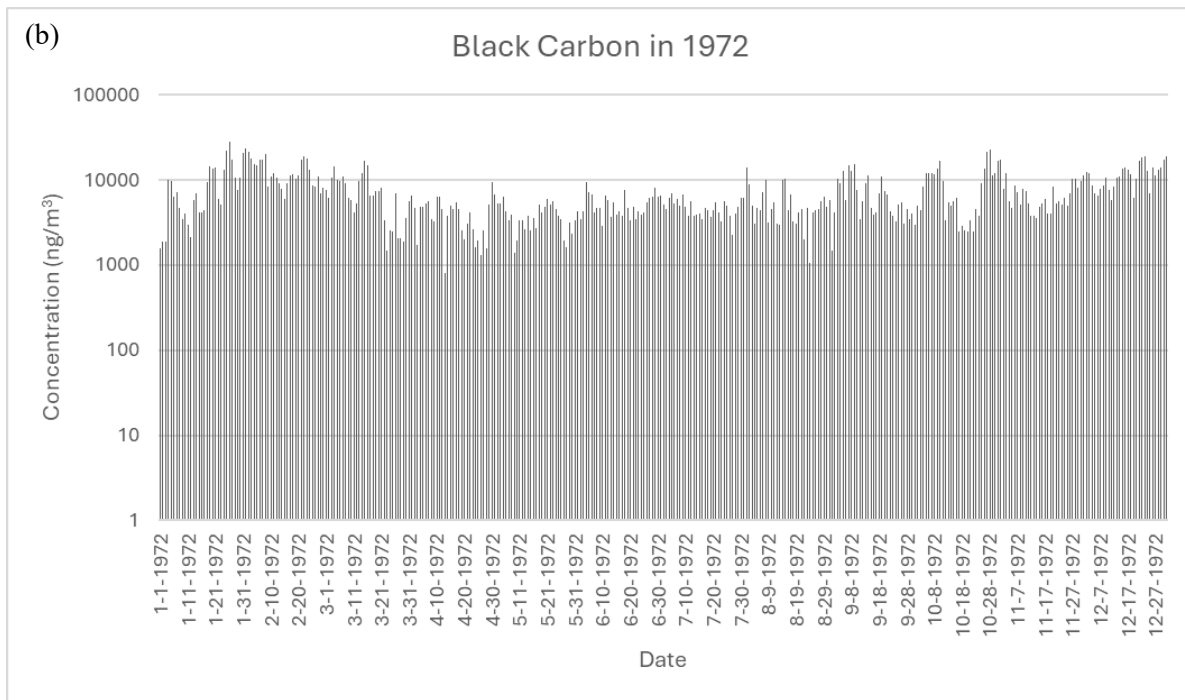
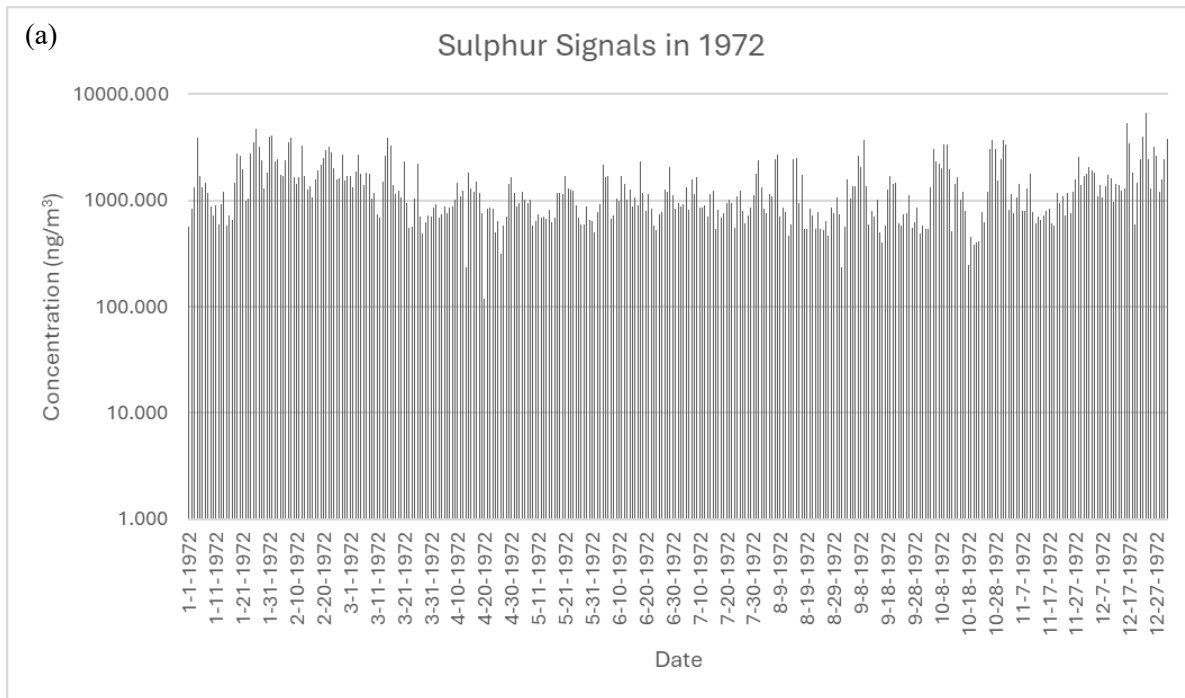
Element	DL	Mean	SD	Minimum	Maximum	N
<b>P</b>	80.83	102.86	47.46	32.88	577.63	365
<b>S</b>	20.09	1365.56	905.46	119.20	6653.15	365
<b>Cl</b>	4.95	1209.13	1516.95	-147.86	22628.67	362
<b>K</b>	3.30	653.66	1569.82	-29.66	23082.79	364
<b>Ca</b>	0.99	4269.09	2374.47	875.99	30374.59	365
<b>Ti</b>	0.99	94.83	94.77	-14.04	951.79	364
<b>V</b>	0.99	41.63	83.41	0.50	473.54	132
<b>Cr</b>	0.82	7.91	50.49	0.81	899.93	118
<b>Mn</b>	1.15	3.35	8.83	1.57	57.55	89
<b>Fe</b>	3.00	409.01	347.26	34.58	2324.47	365
<b>Ni</b>	1.25	30.68	18.52	-1.86	257.96	362
<b>Cu</b>	4.62	35.78	33.46	-3.59	358.10	364
<b>Zn</b>	3.13	176.53	747.47	-5.08	14057.23	364
<b>Ga</b>	1.98	0.21	0.98	1.18	8.57	21
<b>As</b>	0.66	10.45	14.95	1.22	82.65	230
<b>Se</b>	0.66	0.75	1.38	0.59	7.17	132
<b>Br</b>	0.66	50.15	54.76	8.77	646.87	365
<b>Sr</b>	0.99	13.26	24.81	0.13	393.22	365
<b>Y</b>	0.99	2.46	3.53	0.50	32.61	198
<b>Ba</b>	8.25	116.22	63.00	32.33	911.17	365

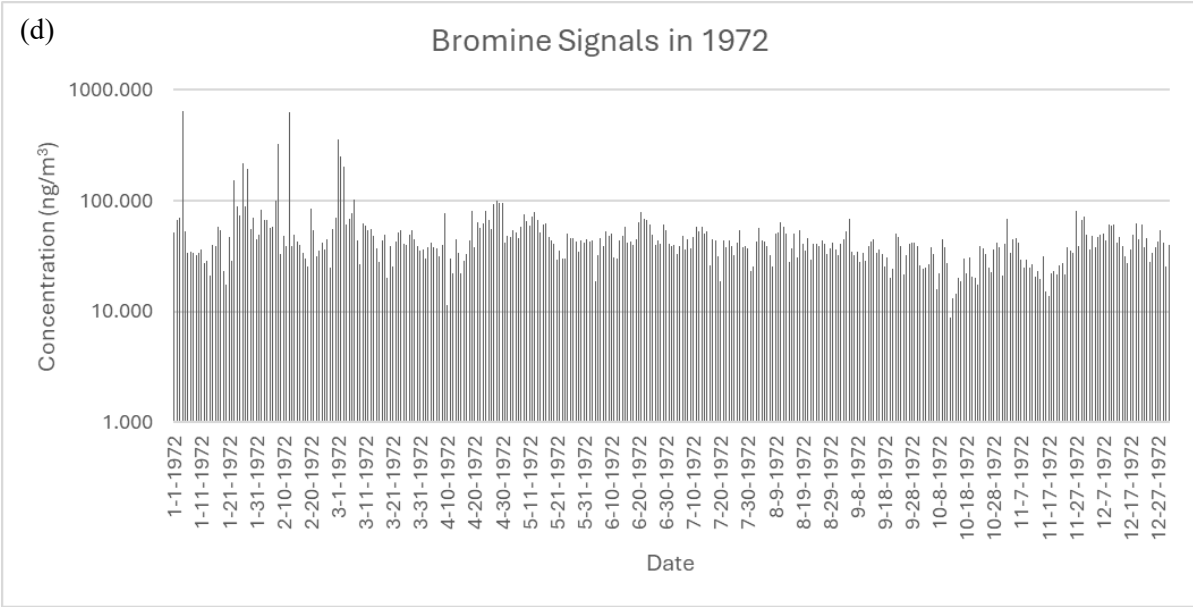
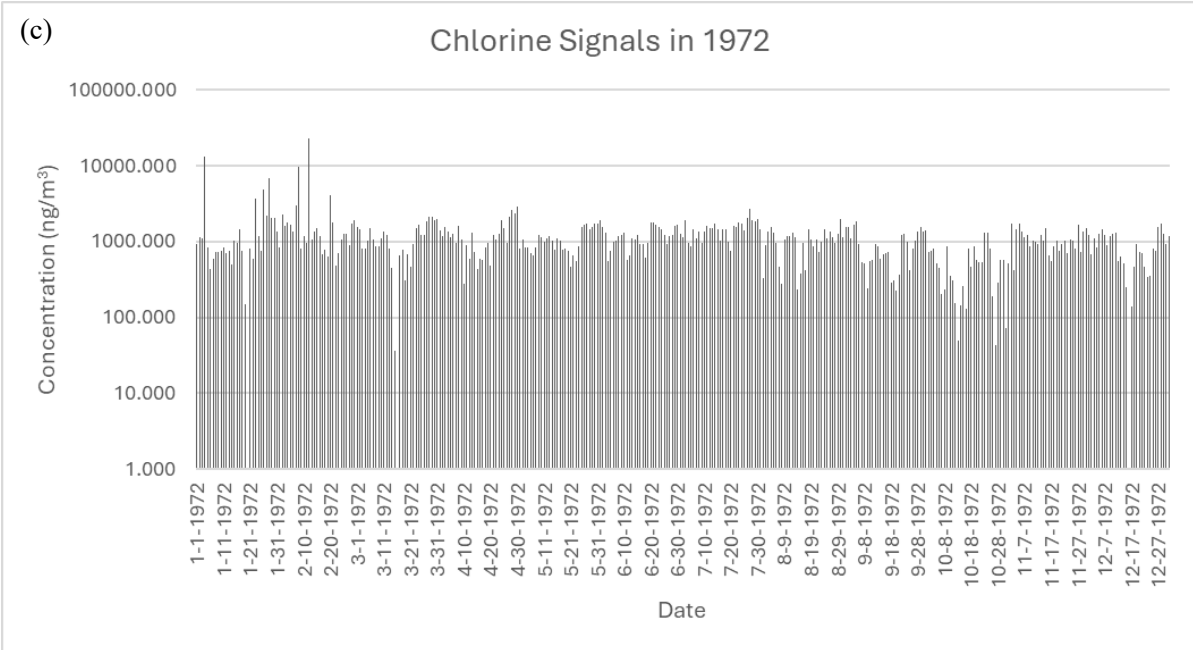
<b>Hg</b>	3.30	1.61	2.54	1.73	32.98	158
<b>Pb</b>	3.30	71.73	93.14	3.63	688.23	288
<b>Bi</b>	3.30	2.92	11.80	2.70	119.22	59
<b>Si</b>	8.25	712.49	712.41	-16.11	4949.55	364
<b>BC</b>	100	7170.80	4637.434.64	809.69	28002.62	365

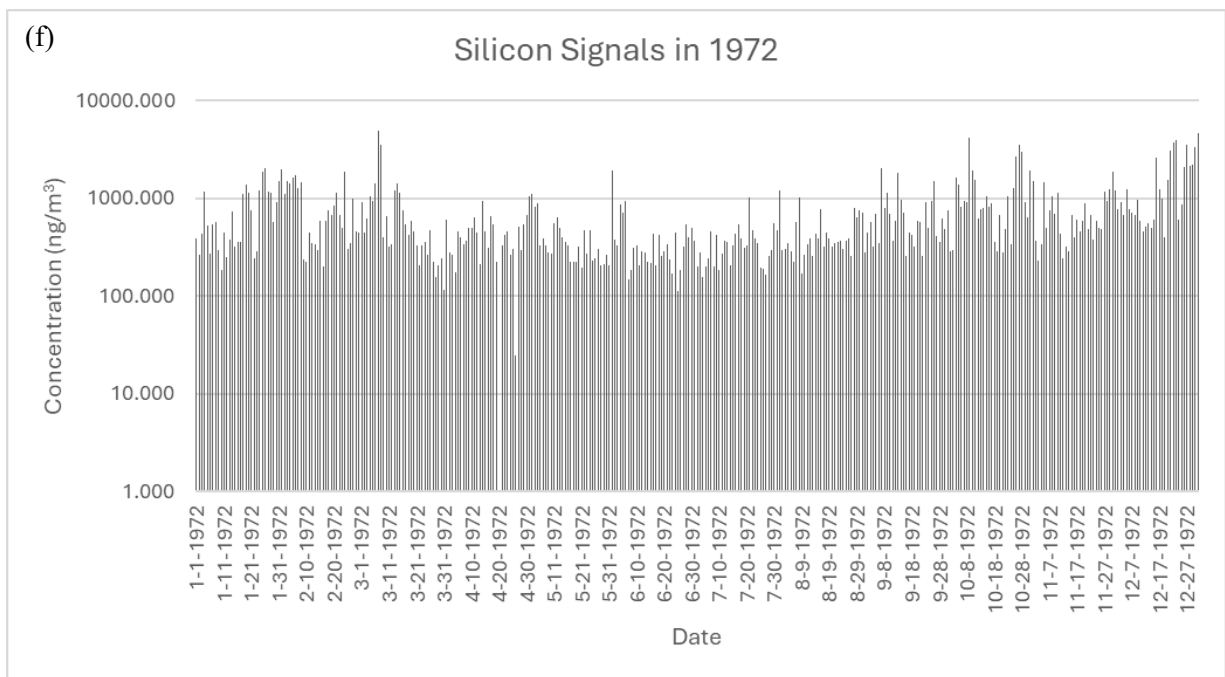
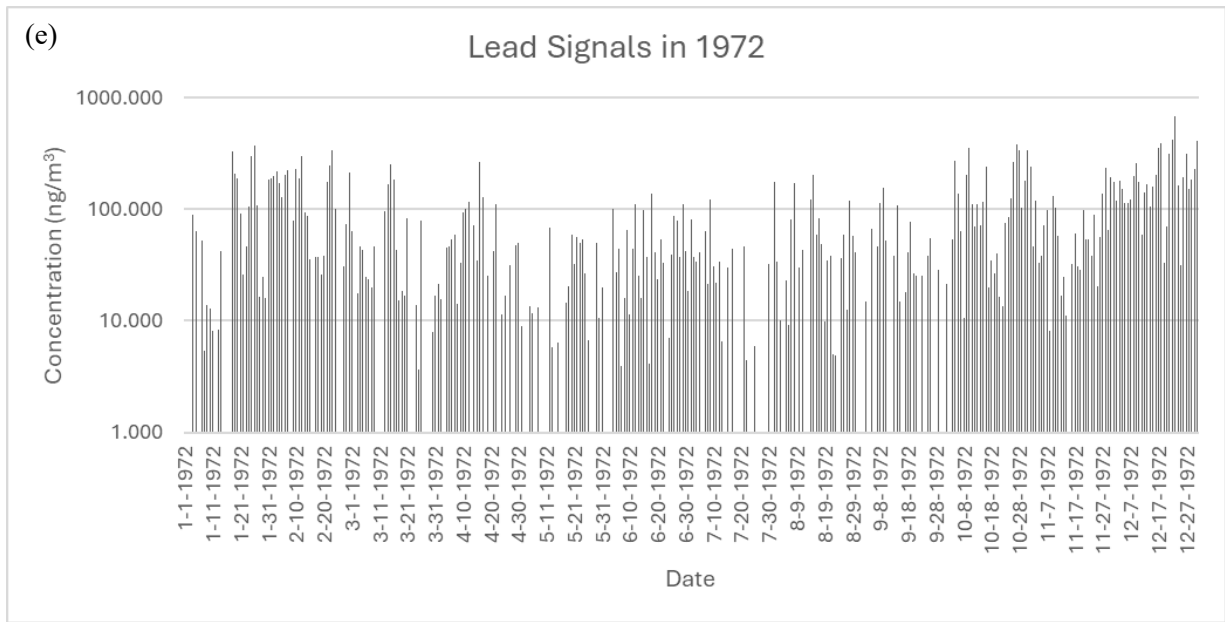


**Figure 3.12:** Time series of elements (in  $\text{ng}/\text{m}^3$ ) characterized by EDXRF from Falsterbo 1972.

The maximum values observed were Ca with  $30374.59 \text{ ng}/\text{m}^3$  (see table 4.1) and the reason for high Ca concentrations was due to the filter paper. One of the main components of the filter paper is Ca, hence, Ca was excluded from the analysis. Hg concentrations were excluded as well due to its volatile properties and the papers were stacked and stored for several years, which means Hg concentrations were not reliable. Few aerosols such as Ga, Bi, Mn, Cr and V had very few signals throughout the year. Elements detected by the EDXRF are mentioned in table 4.1 with their detection limit, mean concentration, standard deviation, minimum and maximum concentration of each element and number of filters in which each element was detected. All element concentration trends observed in 1972 are illustrated in Figure 4.2.







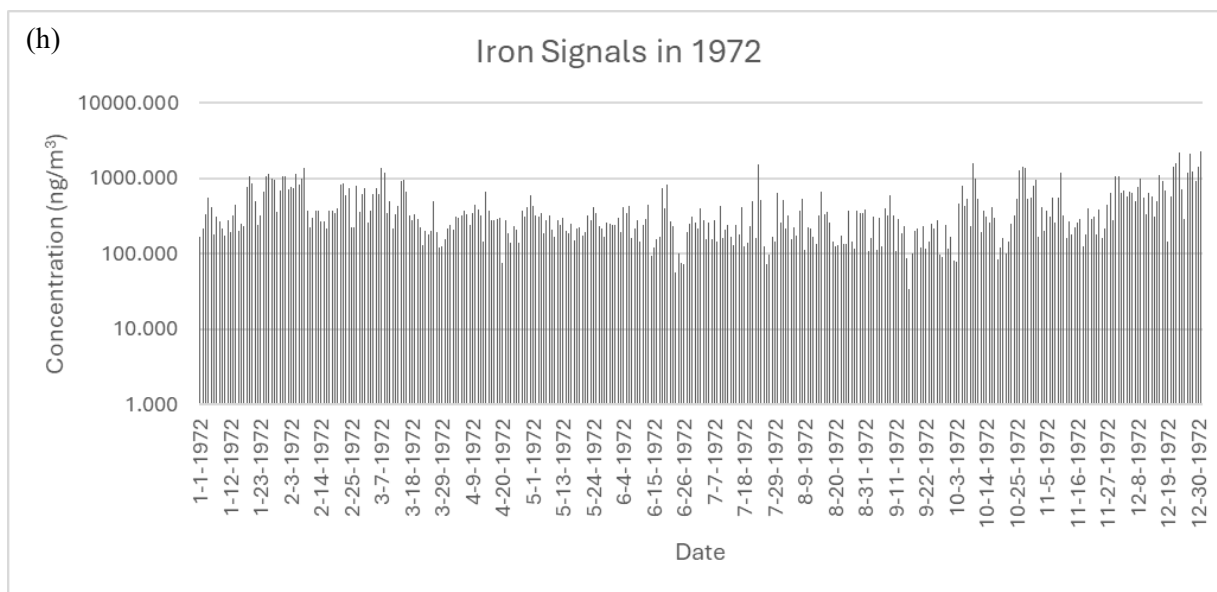
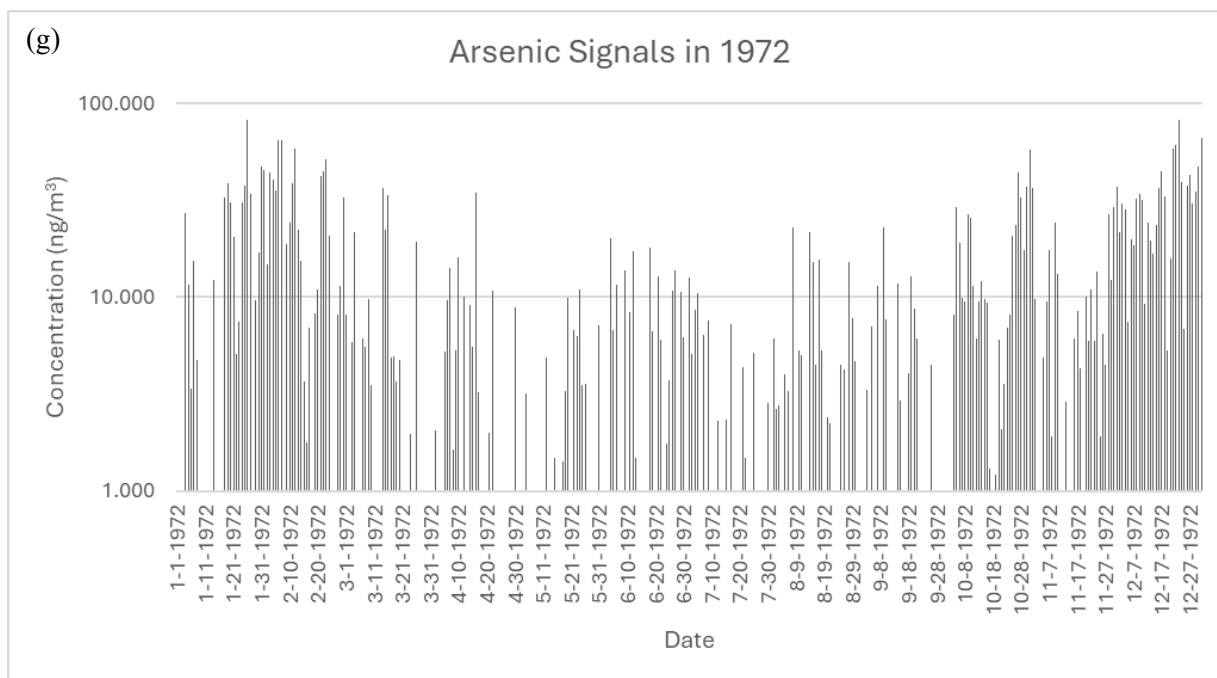
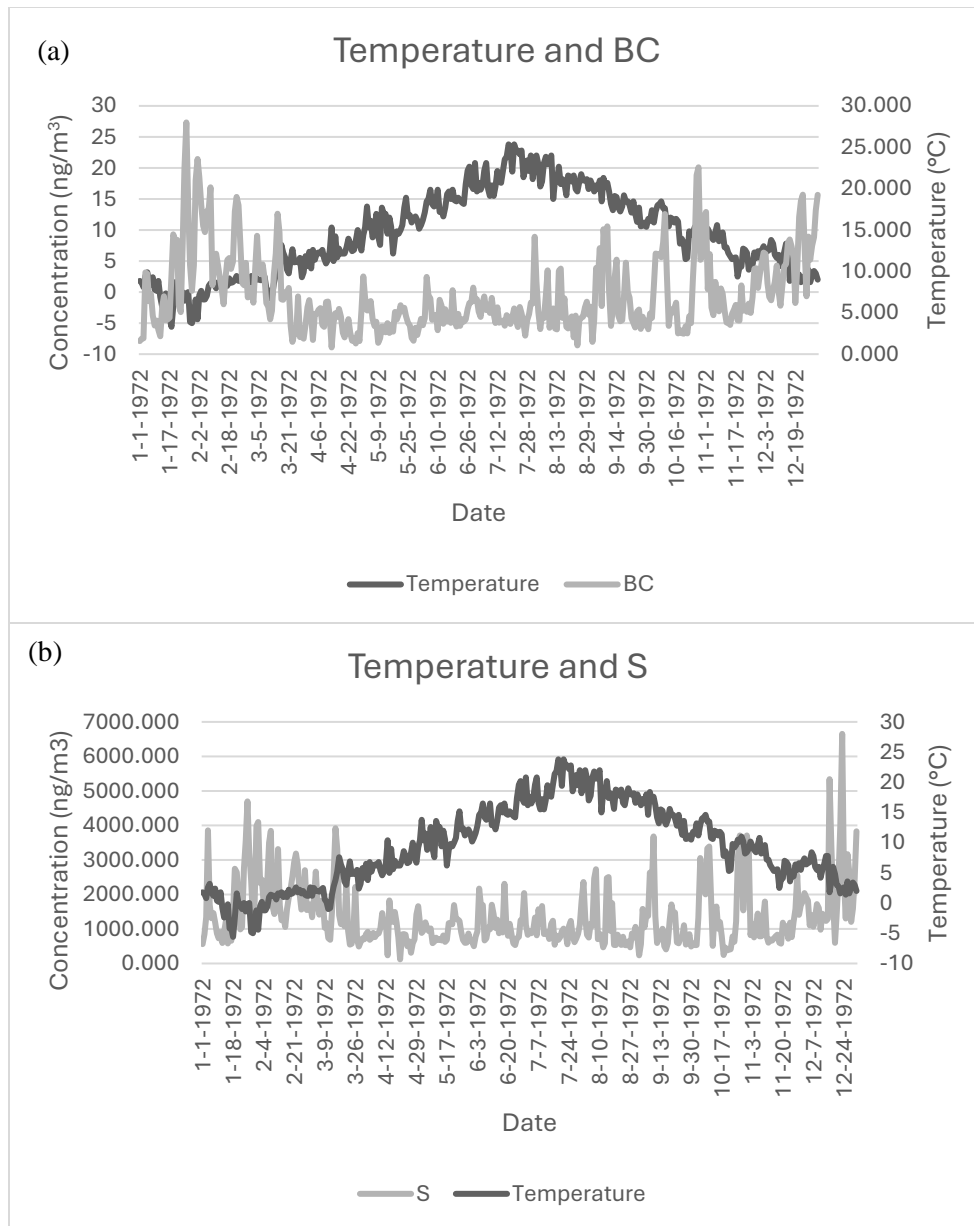


Figure 3.13: (top to bottom) S, BC, C, Br, Pb, Si, Ar and Fe concentrations (in  $\text{ng}/\text{m}^3$ ) as a function of time 1972.

Figure 4.3 shows the aerosol concentration of each element. It is observed that S, BC, Cl, Br, Fe and Si are found in every filter, however, Ar and Pb are found only in a few filters. Table 4.1 shows more details of how many filters had the specific aerosol.

Cl and K were at their highest peak on 2-12-1972, and it is assumed that the filter on that day has been contaminated with other sources during handling or nearby wood burning in residential area. However, it is not possible to predict exact possibilities of contamination.



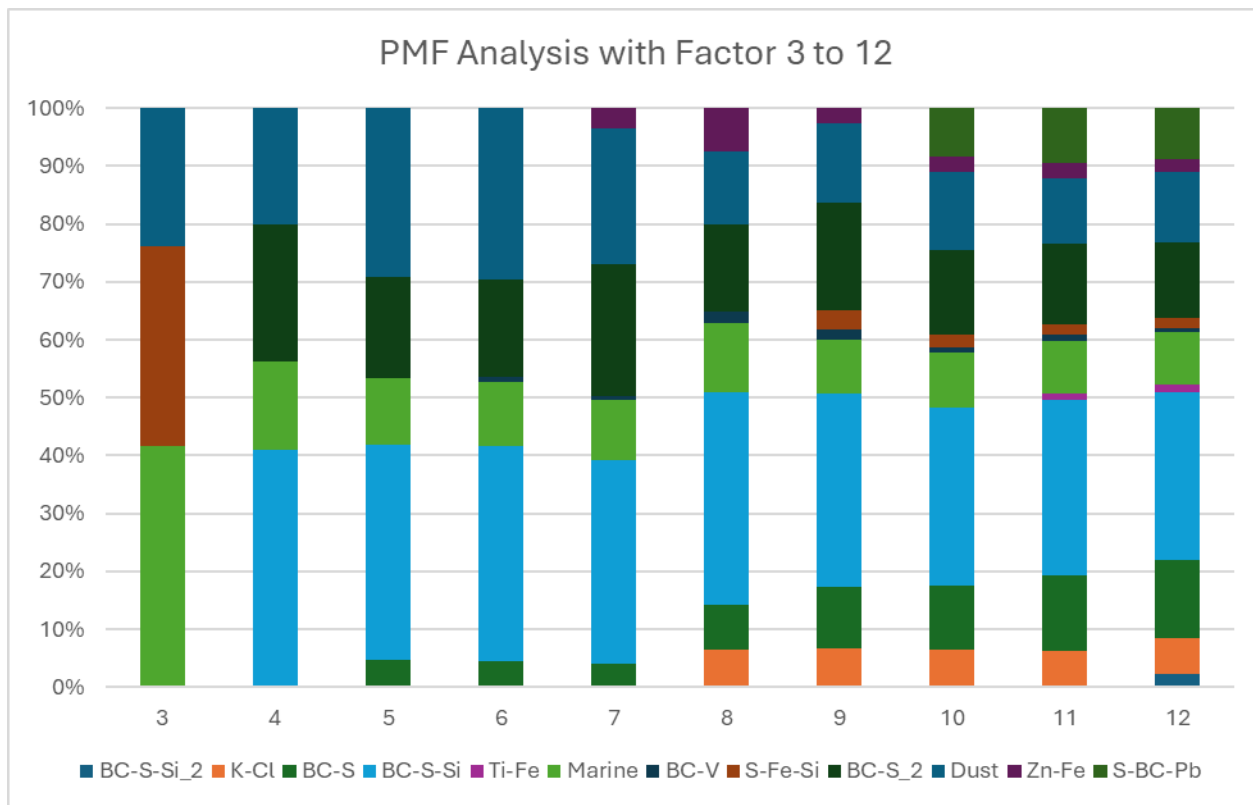
**Figure 3.14:** (a) BC and (c) S concentration (in ng/m<sup>3</sup>) correlated with temperature (in °C) as a function of time 1972.

As suspected, BC and S concentrations increased during winter and decreased during summer. This is due to coal, wood or biomass burning during winter for heating purposes in residential areas that increased BC and S concentrations in the atmosphere. More correlations were conducted by PMF analysis, which gave a more robust scenario of the source factors of these aerosols.

### 4.1.3. Results from PMF Analysis

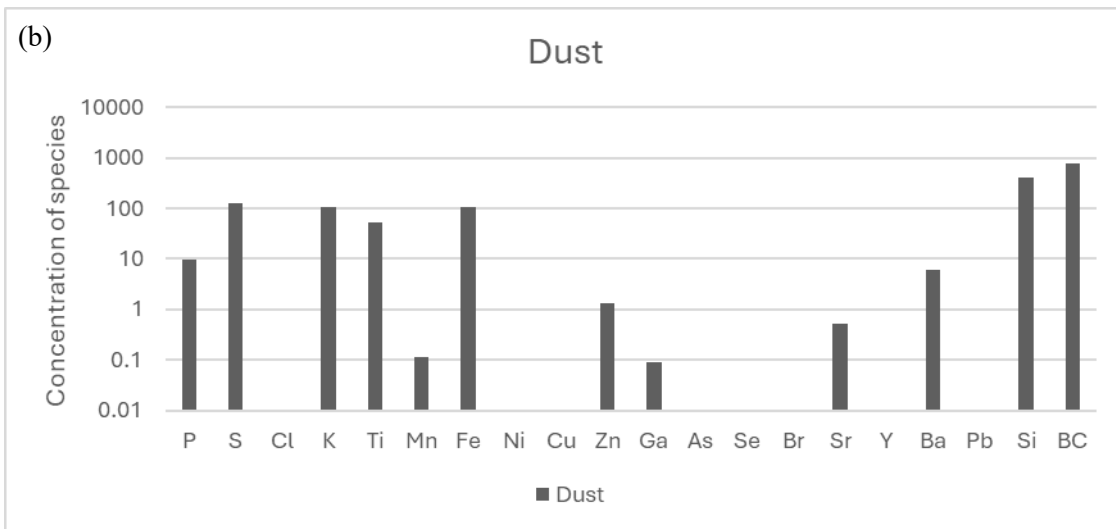
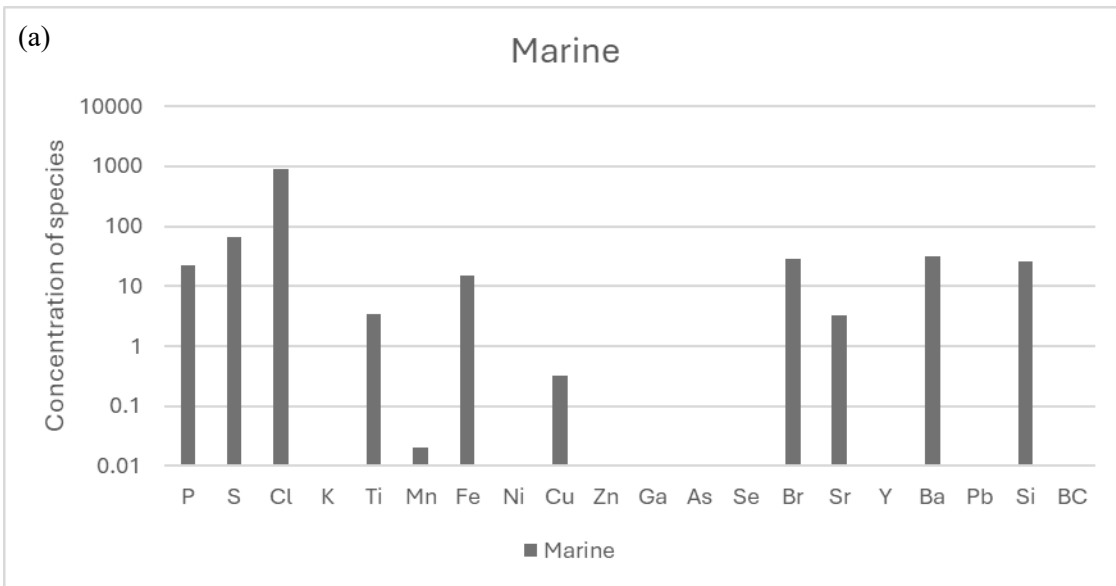
PMF analysis was run 20 times with an increasing factor number from 3 to 12, producing 10 different solutions of factor plots with the aerosol concentrations. These solutions were then

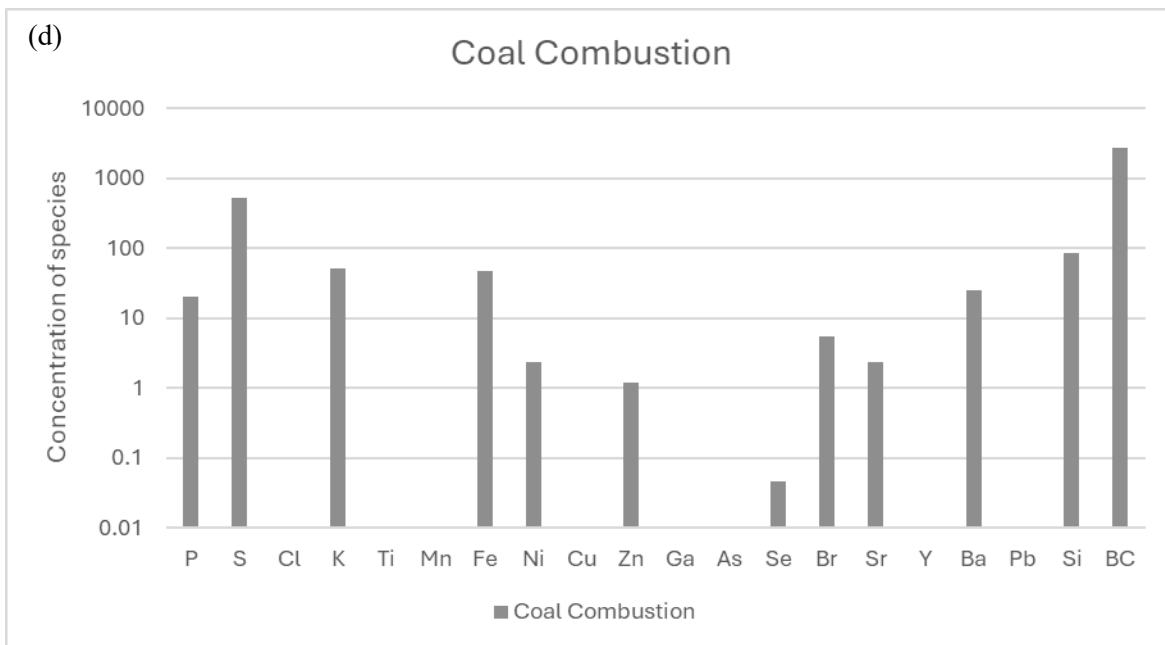
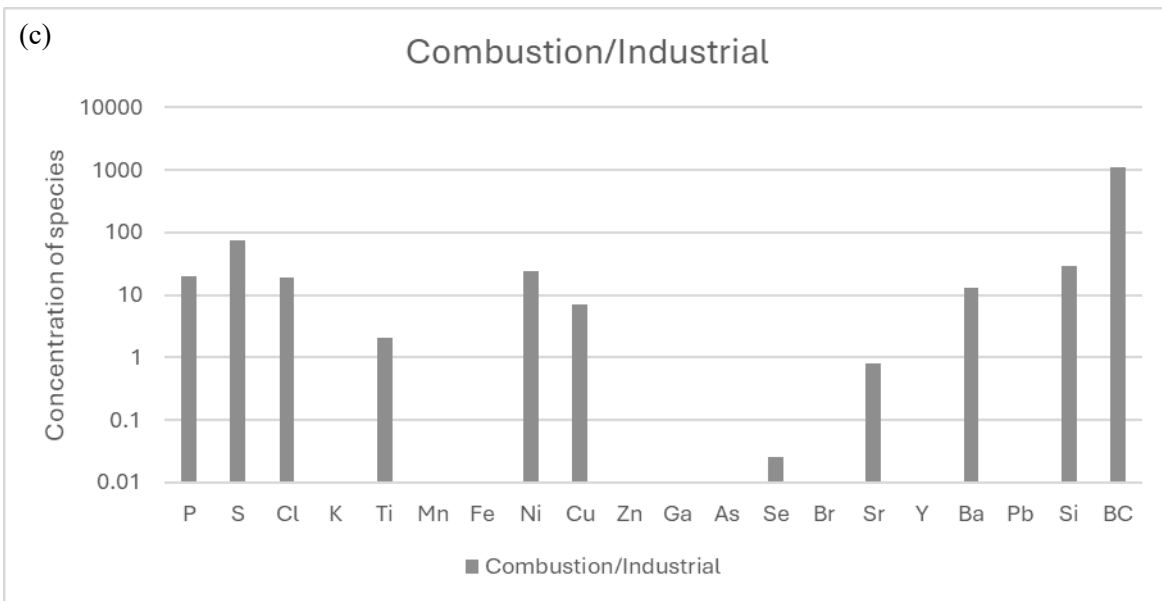
compared with each other and the solution that showed the most stable factors was then selected for detailed analysis and source apportionment to determine the source of the aerosol emissions. Figure 4.5 shows the solution of factors. Factor 10 shows the most stable factors compared to the other solutions from 3 to 12.

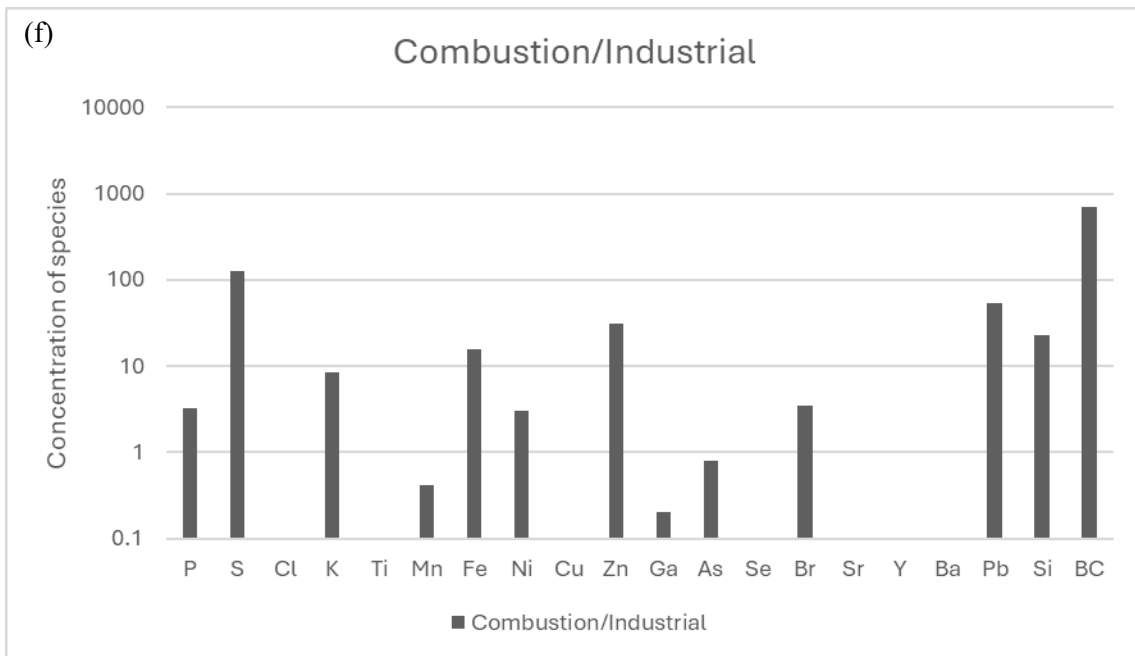
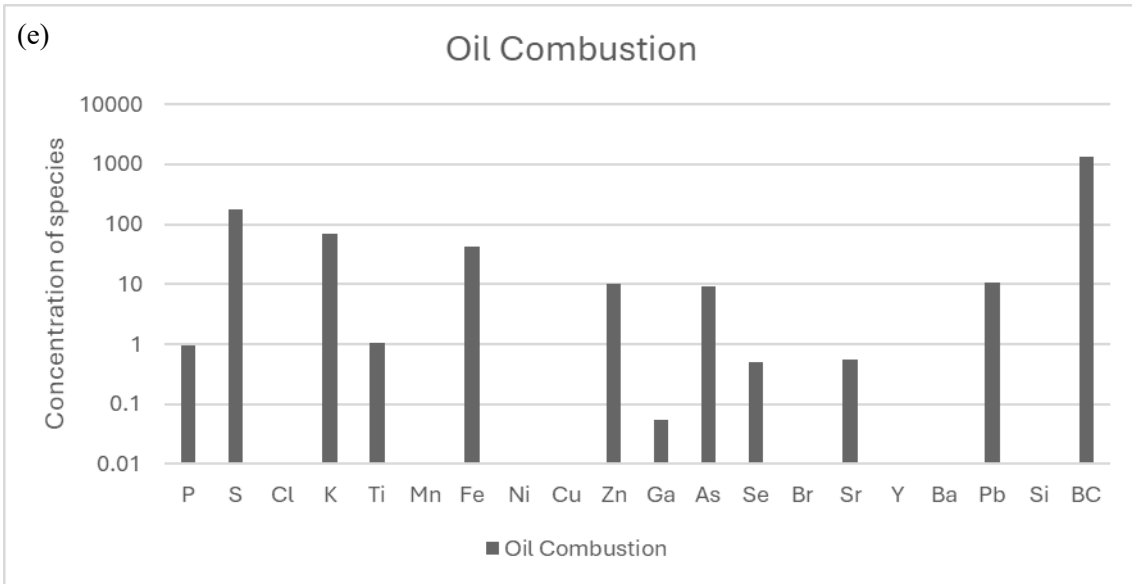


*Figure 3.15: Solution of factors from 3 to 12.*

Source apportionment was done by considering the aerosols with highest concentration peak from each plot. The plots were compared and the elements with highest concentration signals from each plot were correlated. The source of these aerosols was then compared with literature from studies that were done before regarding type of element and the source of emission in the atmosphere.







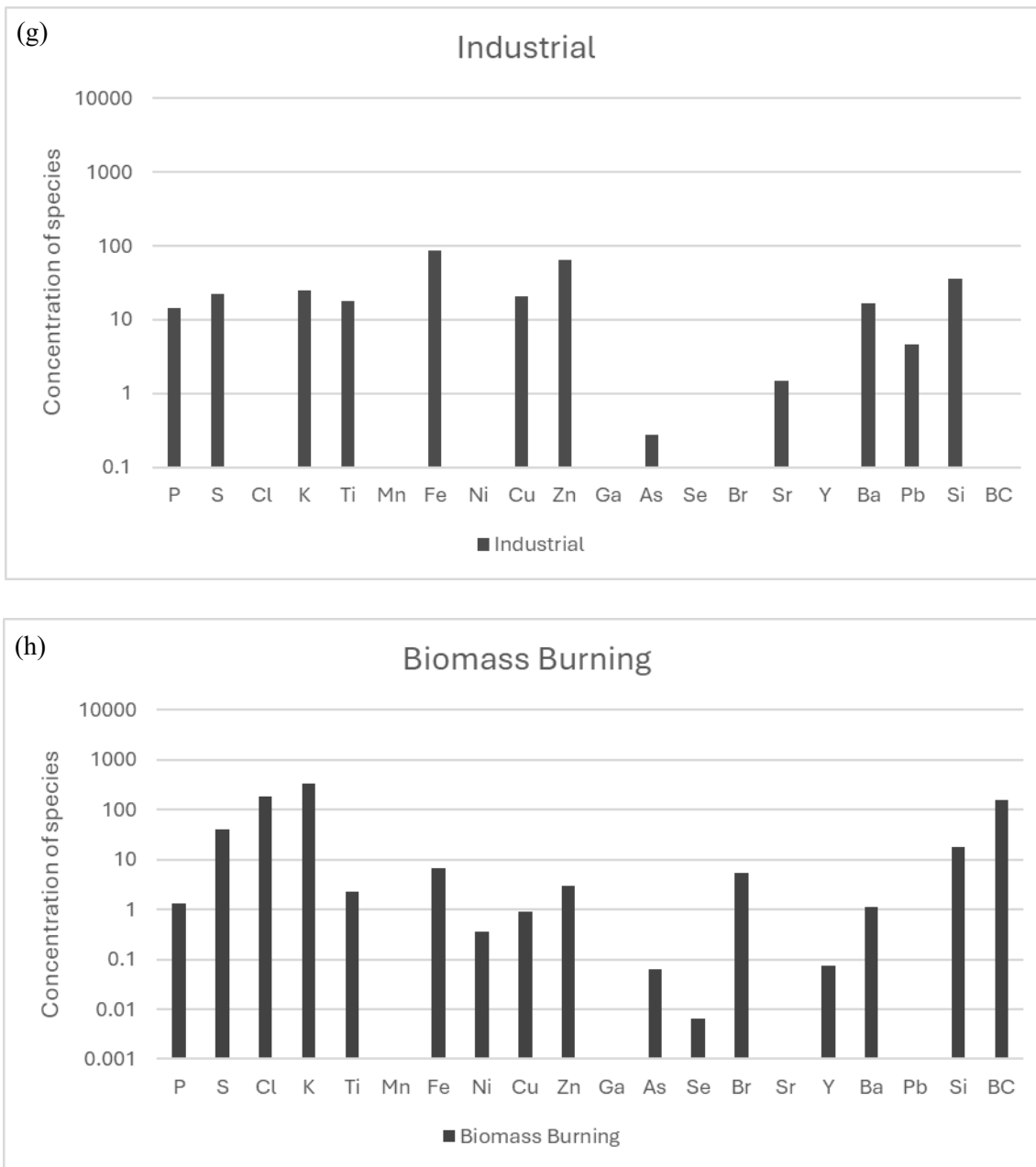


**Figure 3.16:** PMF analysis with Factor 3 to 12, (a) marine s, (b) dusts, (c) combustion/industrialization (d) coal combustion, (e). Oil combustion, (f) combustion/industrialization, (g) industrial, (h) biomass burning.

The plots were compared and the elements with highest concentration signals from each plot were correlated and compared with literature from previous studies. In Figure 4.6, plot (a) shows high concentration of Cl and Br, which indicates the source factor might be salt water (Calvo et al., 2013). Plot (b) shows the highest signals from Si and BC, which indicates dust with mix of biomass burning. Plot (c) and plot (f) shows high signals of BC and S indicating combustion or

industrialization, and coal and oil combustion in plot (d) and (e) respectively (Johnsen & Rasmussen, 1977).

A few aerosol elements such as Mn, Sr, As, Ba, and Ti were not represented well in the PMF model. However, it can be illustrated that most air mass entering Southern Sweden in 1972 had large proportion of aerosols produced from dust, coal combustion, biomass and oil burning and marine aerosols. As Falsterbo is a rural area with less industrial activities, long-range pollutants derive from biomass burning, coal and oil combustion, industrial activities, and dust and marine aerosols. However, it is expected that marine aerosols will be high as Falsterbo lighthouse resides in the Southern coastal region. Furthermore, HYSPLIT analysis gave a clearer illustration of these aerosol sources.

#### 4.1.4. Results from Air Mass Trajectory Analysis

HYSPLIT software was used to find mean cluster trajectories for 1972 that reached Falsterbo. The percentage of trajectories coming from other parts of Europe to the receptor site Falsterbo lighthouse was calculated. The clusters also gave an illustration of the distance and direction of the air masses reaching Falsterbo.

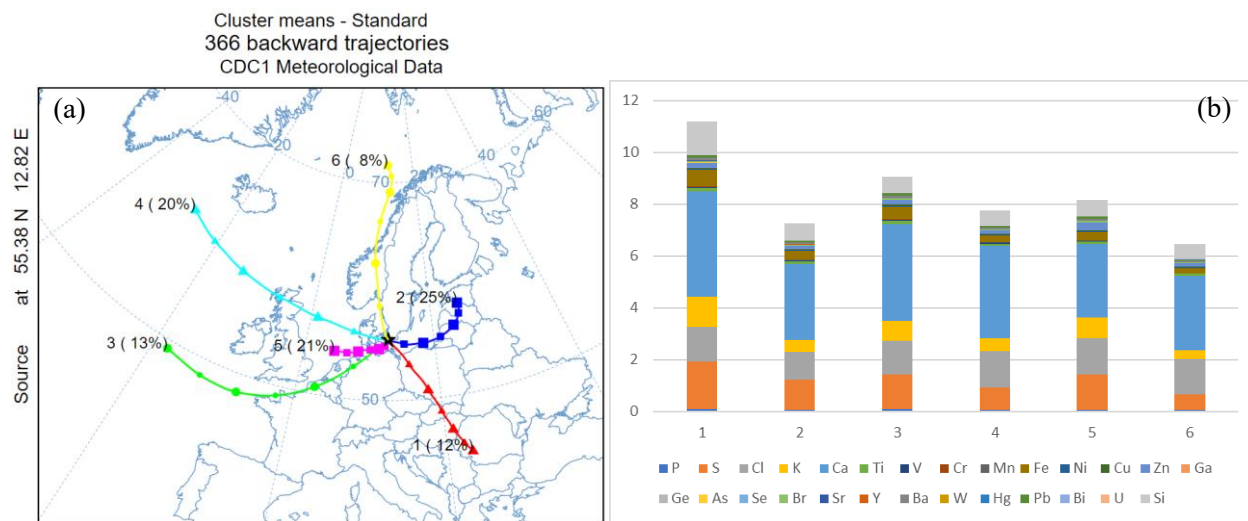
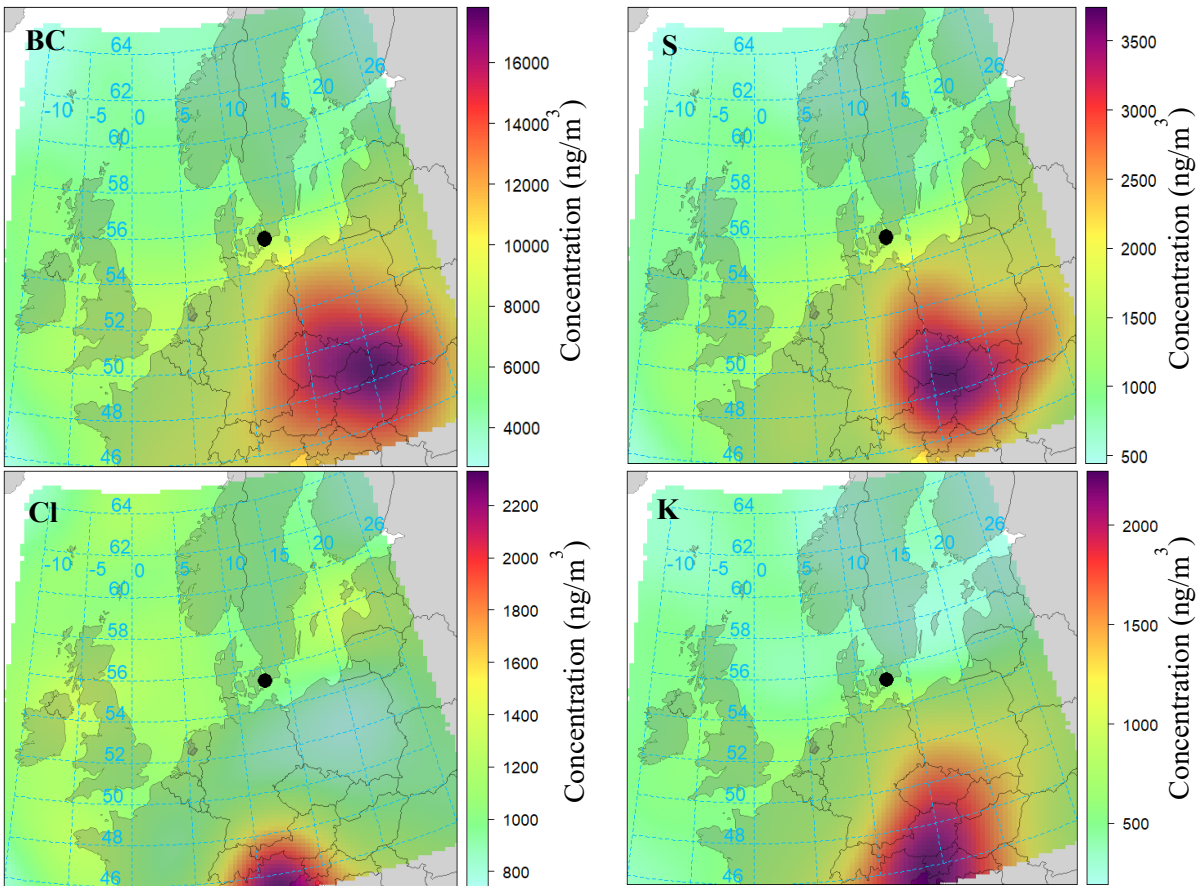


**Figure 3.17:** (a) mean clustered air mass back trajectory entering Falsterbo in 1972 (total run time: -72 hr), (b) Element concentrations in each cluster.

Total of 6 mean clusters were selected and run in the HYSPLIT model with total run time of -72 hours per day. In Figure 4.7 illustrates the concentration of element with respect to each mean cluster back trajectory. For example, S is high in cluster 1, and 12% of the air mass entering

Falsterbo comes from the eastern Europe. Additionally, Cl concentration is high in cluster 4, and 20% or air mass entering Falsterbo comes from the North Sea and Atlantic ocean.

Concentration weighted trajectory (CWT) technique was then conducted using openair R studio. CWT technique employs a grid domain based on calculating concentration fields to pinpoint places where pollutants originate (Seibert et al., 1994). This technique is similar to the Potential Source Contribution Function (PSCF) which determines the probability of a source being situated at a certain latitude and longitude (Fleming et al., 2012; Pekney et al., 2006), and is commonly used in air mass back trajectory analysis. However, the PSCF approach has a drawback because grid cells can provide identical PSCF values regardless of whether sample concentrations are either marginally above or much greater than the criteria (Hsu et al., 2003). This presents a difficulty in distinguishing between sources that are moderately reliable and those that are very reliable. CWT technique addresses this problem of PSCF by differentiating between moderate and strong sources.



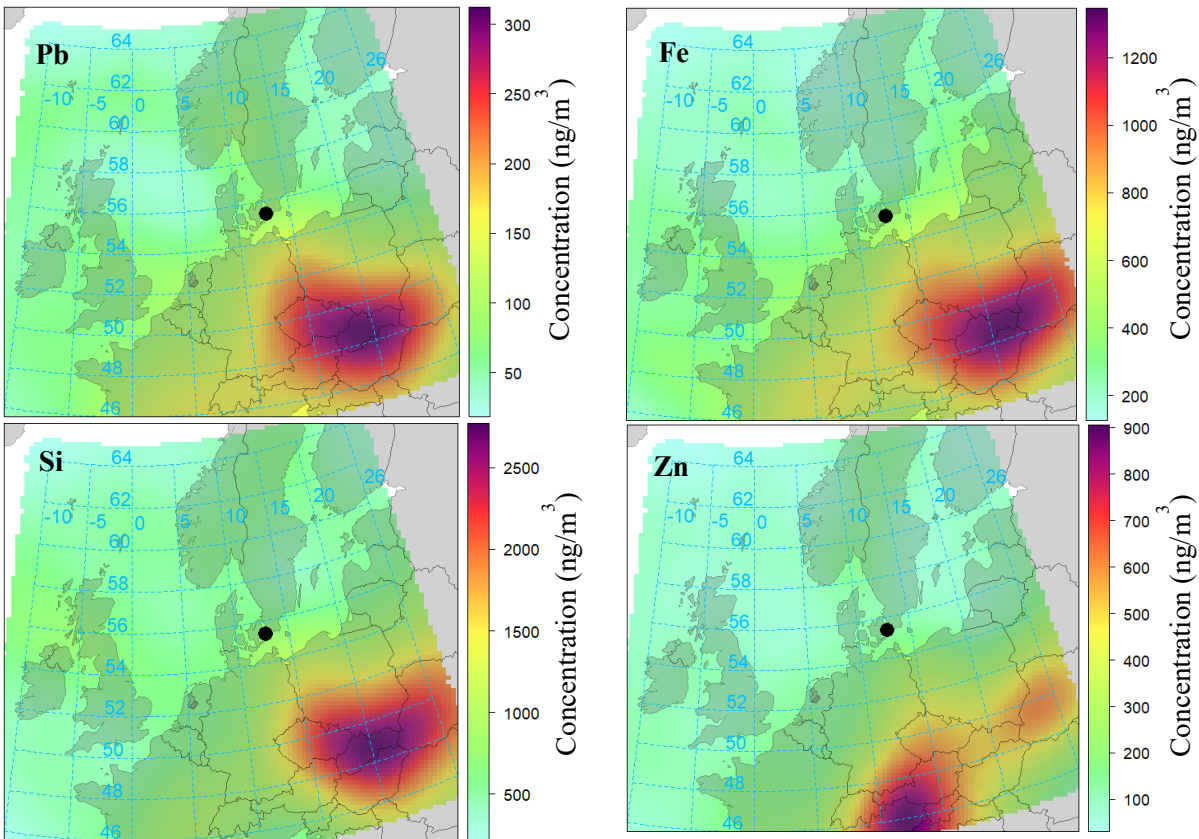
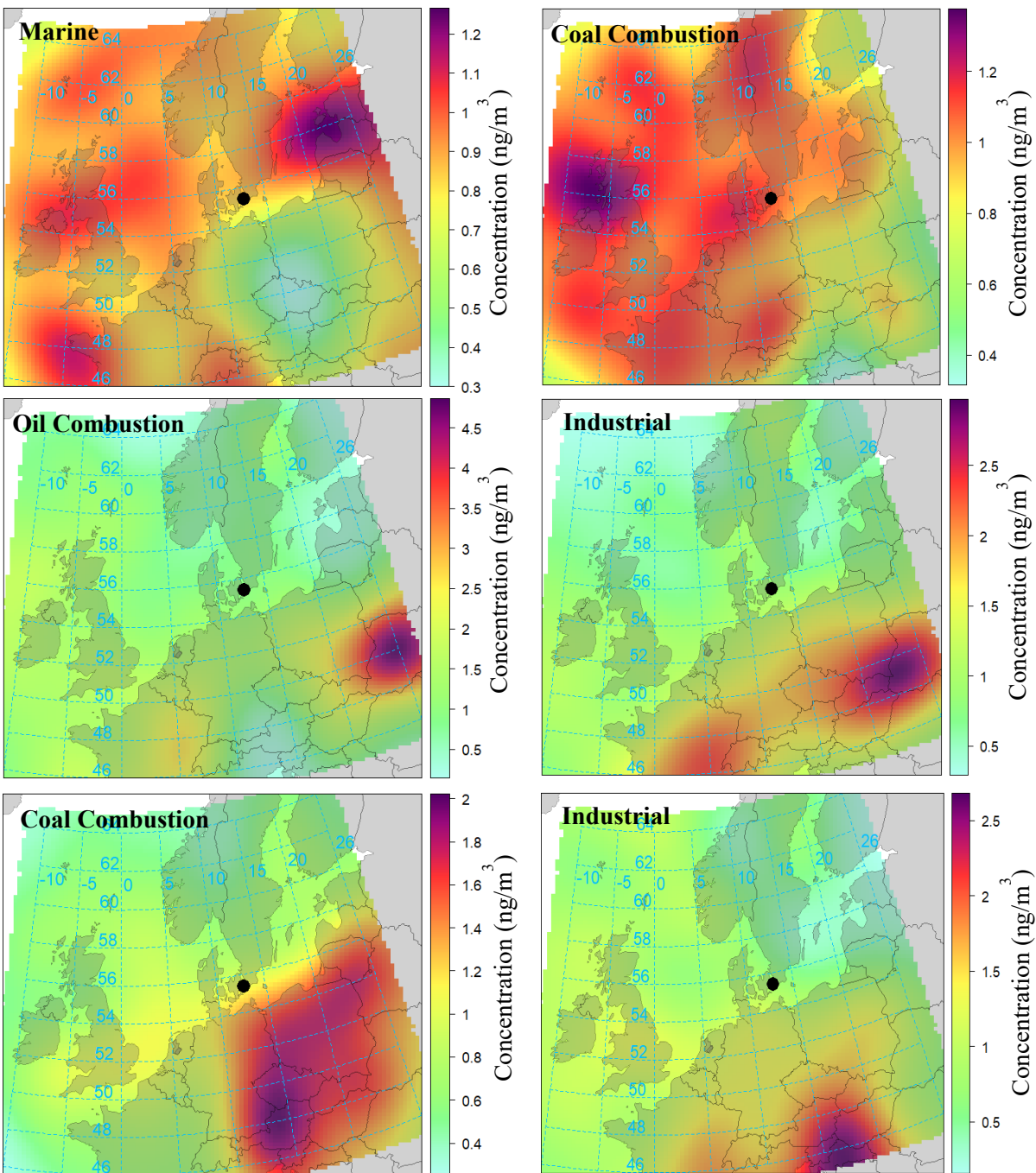


*Figure 3.18: CWT technique with element concentration (in  $\text{ng/m}^3$ ) and their respective region of Europe.*

Air mass back trajectories shown in Figure 4.8 illustrate the pattern of air mass with the aerosol concentration it carries. The higher aerosol concentration regions in red are the point of origin from where the aerosols have been emitted and entered Falsterbo in 1972.

Figure 4.8 shows that BC is mostly seen to come from Slovakia, northern Hungary and some concentrated traces from Czech Republic to Southern Sweden. S shows similar trends but more concentrated from the Czech Republic and Austria. Cl is highly concentrated from Italy and K is concentrated mostly from Italy and Slovenia. Pb is seen to be more concentrated from the Northern Czech Republic and also from Slovakia, and K is seen to be more concentrated from Slovakia and eastern parts of Czech Republic. Fe and Si are seen to have similar air masses and similar source areas from Slovakia and Hungary. Pb is highly concentrated in Slovakia and eastern Czech Republic, explaining that Pb ban legislations were not implemented in these countries during 1970s, and Zn is highly concentrated from Italy.

CWT technique was combined with PMF source apportionment to understand the concentration trajectory of each factor in this study and illustrate the source factors with the back trajectories entering Falsterbo.



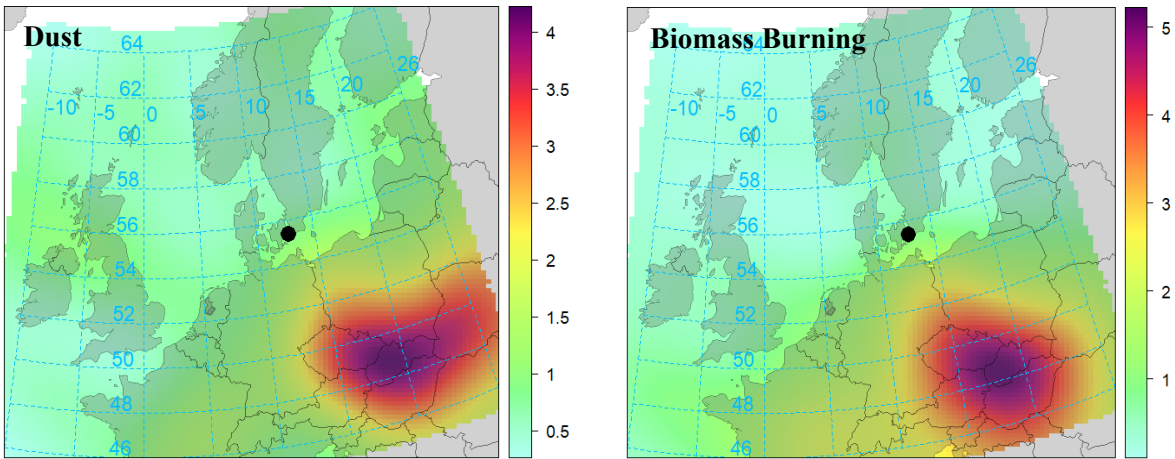


*Figure 3.19: CWT technique with element concentration (in  $\text{ng}/\text{m}^3$ ) with source factor and their respective region of Europe.*

According to Figure 4.9, marine source factors are highly concentrated from the Baltic and the North Sea. This gives more concrete evidence that the source factor is in fact a marine and Cl and Br are marine aerosols. High concentrations of coal combustion can be seen to be from Great Britain, Northern Austria, Czech Republic and some parts of Poland. Industrial emissions can be seen high from Hungary and Croatia. Dust aerosols are highly concentrated from Slovakia, eastern Czech Republic and northern Hungary. Biomass burning is highly concentrated from Slovakia, Czech Republic and eastern Hungary. And finally, oil combustion is highly concentrated from Ukraine. In summary, most long-range pollutants from coal combustion, industrial activities, biomass burning, oil combustion and dust mainly enter Falsterbo from Eastern and Southern Europe, and also from UK.

This study was later compared with other studies regarding industrial activities in Europe. Czechoslovakia, for example, in the 1970s was at its peak in industrialization after World War II and that shows higher trends in coal powered powerplants during the 1970s (Nielsen, 2017). This justifies the high concentration of BC and S from northern parts of Czech Republic (formally Czechoslovakia) that can be observed in the cluster back trajectories.

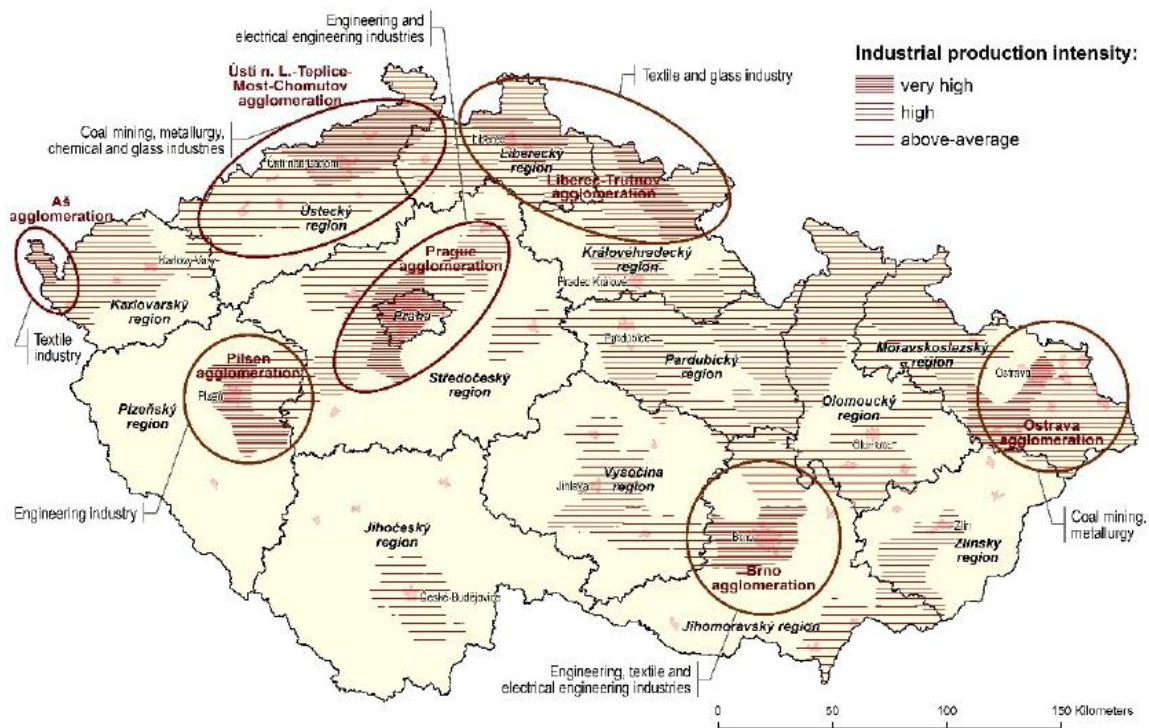


Figure 3.20: Industries in Czechoslovakia (Kunc et al., 2018).

Figure 4.10 shows that most coal mining and industries were abundant in the northern part of Czechoslovakia. During that period, Czechoslovakia flourished with industrialization more than any other European country. Coal mining was the main source of energy for the nation and increased coal mining was recorded in the 1970s and 1980s. Similar industrial activities were recorded from East Germany and Poland.

## 4.2. Preliminary Assessment

After conducting initial assessment of 1972, it was concluded that these filters contained aerosol concentrations that can be analyzed in detail. Hence, preliminary assessment was conducted. For this assessment, EDXRF analysis was primarily used. Every eighth filter was selected in the time series to reduce the sample size.

At least three different kinds of filters (see Figure 4.11) were used throughout the time from 1966 to 1990, and it is expected that different filters will have different composition of elements. Due to different types of filters, it was not possible to use the blanks from 1971 and 1978. Instead, the lowest concentration of each element was considered as a background.

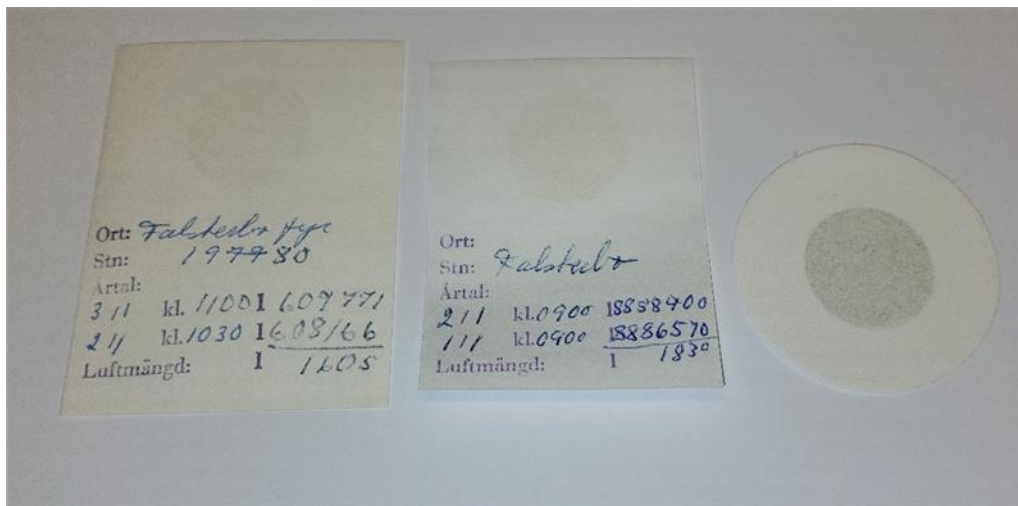
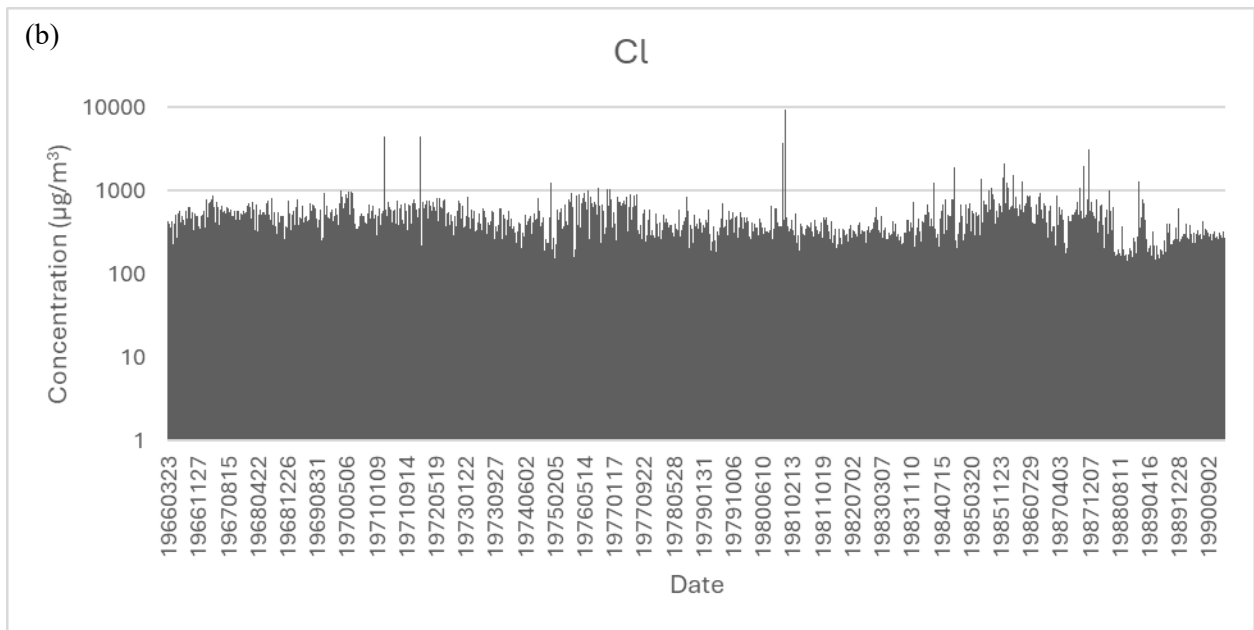
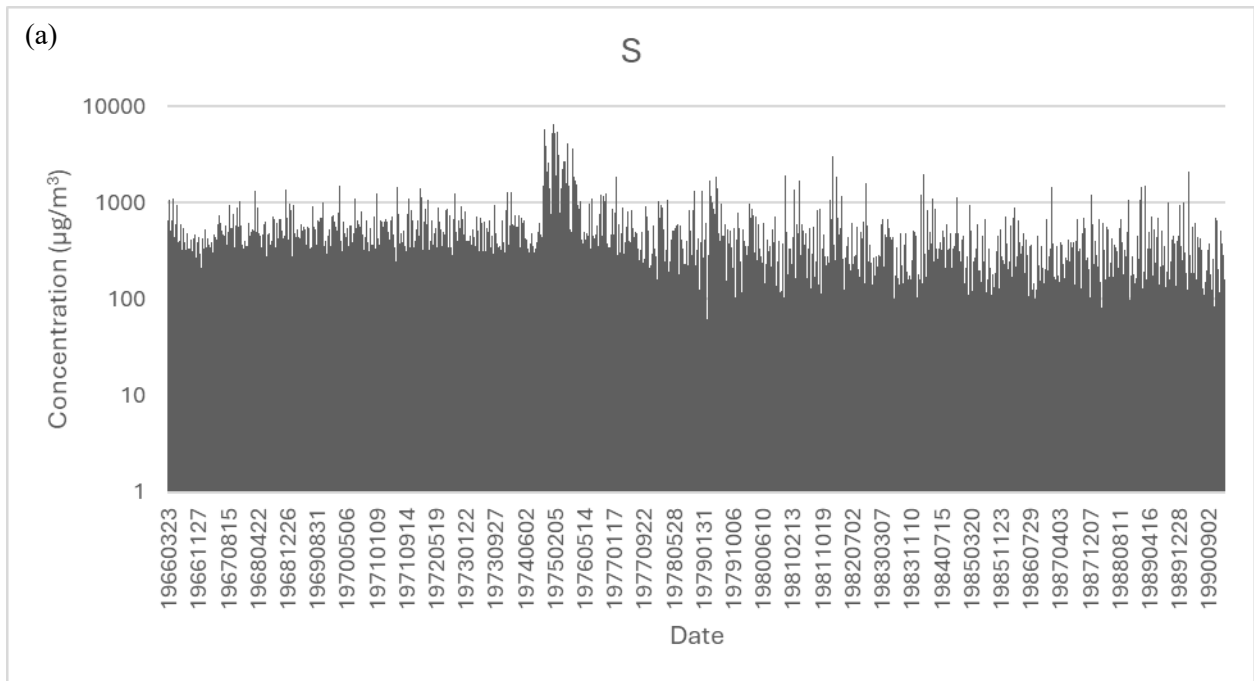
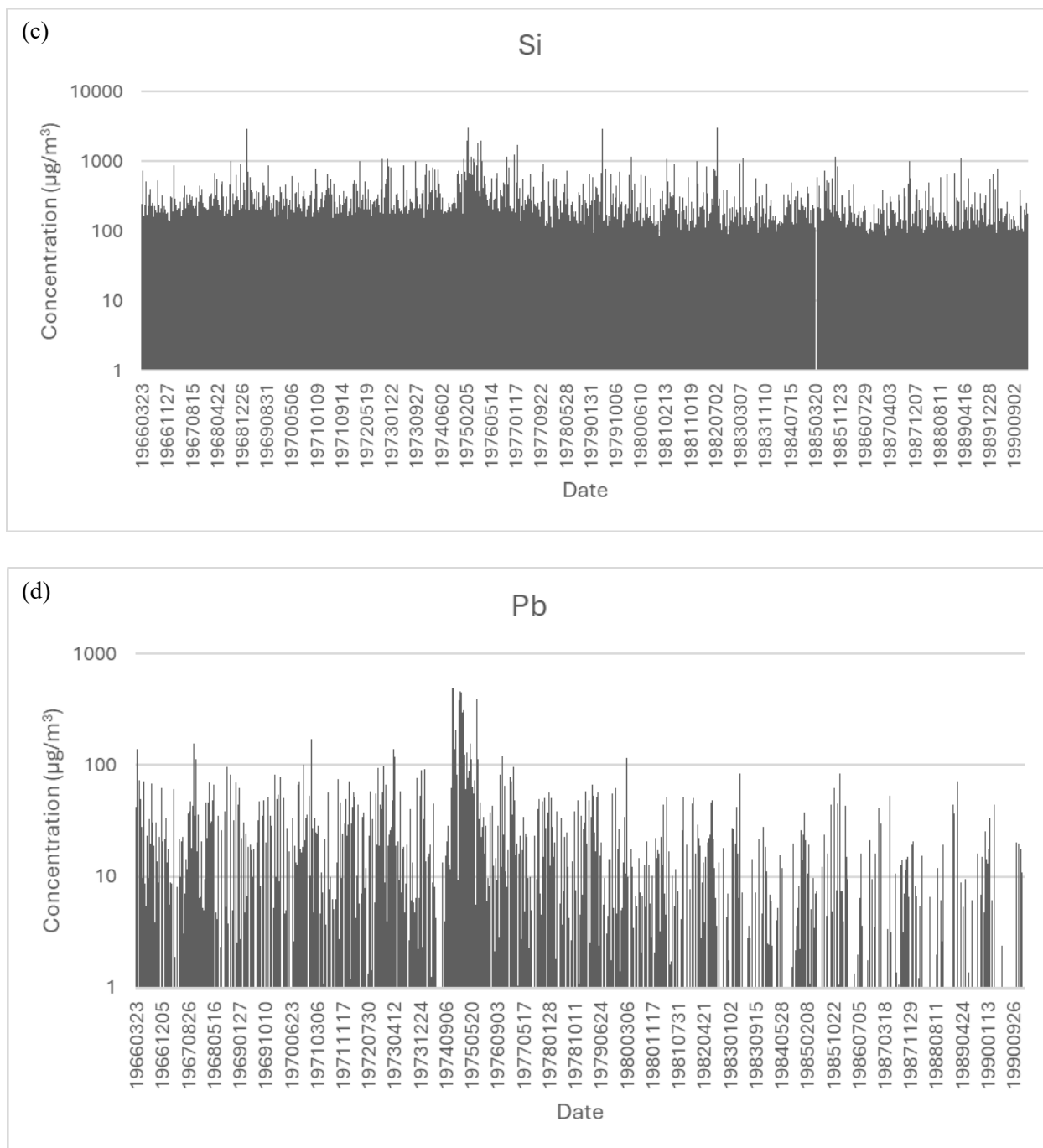


Figure 3.21: Different types of filters from 1966 to 1990.





**Figure 3.22:** Aerosol concentration (in  $\mu\text{g}/\text{m}^3$ ) in the function of time 1966 to 1990.

Figure 4.12 shows the concentration trend of S, Cl, Si and Pb from 1966 to 1990. The variation of the aerosol and reduction in concentration of Pb as a function of time can be observed from the plot above. Further characterization of aerosols with 24-hour resolution can be achieved as the archived filters contain aerosol concentration signals preserved for detailed study.

Furthermore, to characterize the concentration of the elements on a yearly basis, mean element

concentrations were calculated per year to study the differences in concentrations per year (see Figure 4.13).

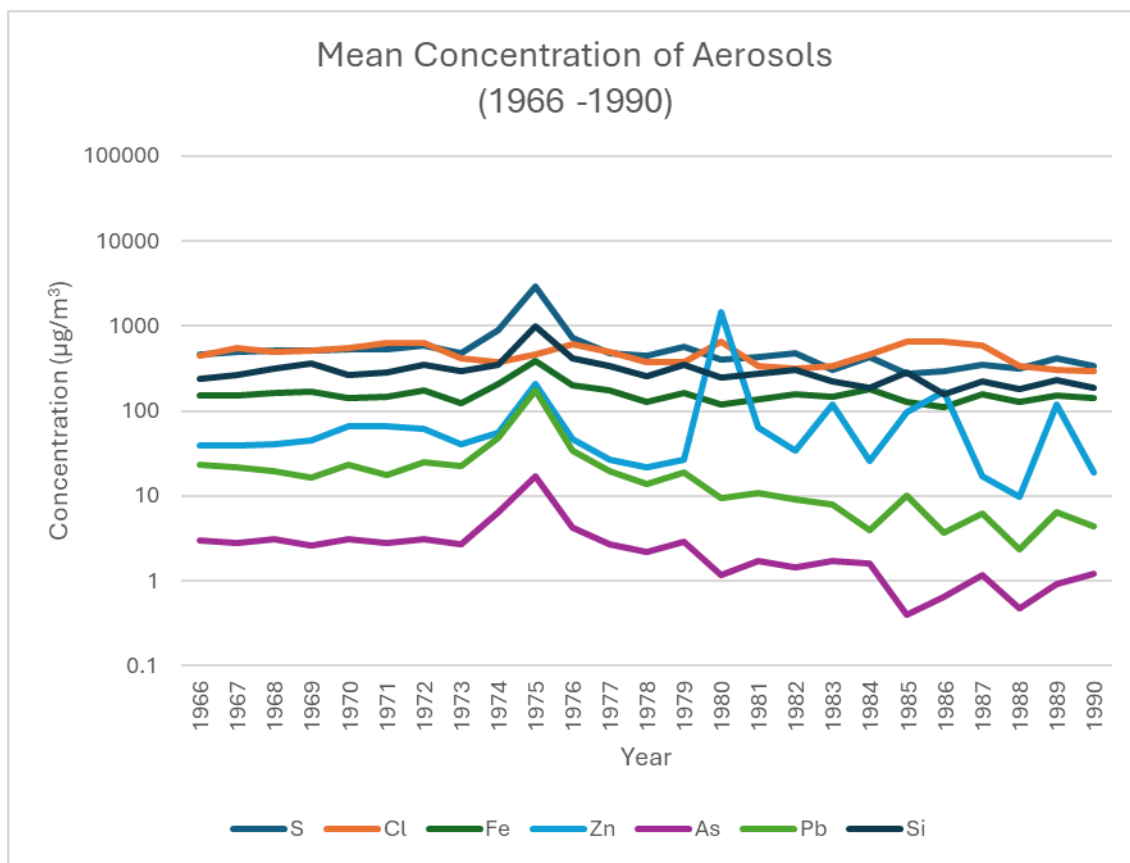


**Figure 3.23:** Mean concentration (in µg/m³) per year of S, Cl, Fe, Zn, As, Pb and Si from 1966 to 1990.

Figure 4.13 shows that the concentration of As and Pb decrease from 1970s and onwards, however, S, Cl, Fe and Zn do not show any reduction in mean concentration. This explains that legislation to regulate air pollution has been in effect since the 1970s, however, from Figure 4.12 it can be seen that the concentration of Pb is still present in Falsterbo. This suggests that further air mass back trajectory analysis, followed by PMF analysis can be conducted for these years to understand the long-range air pollutants.

Another study was conducted by (Hoesly et al., 2018) shows BC emissions per year from various European countries, and data from this study can be compared with Falsterbo to have more concrete evidence of long-range air pollutants from various parts of Europe.

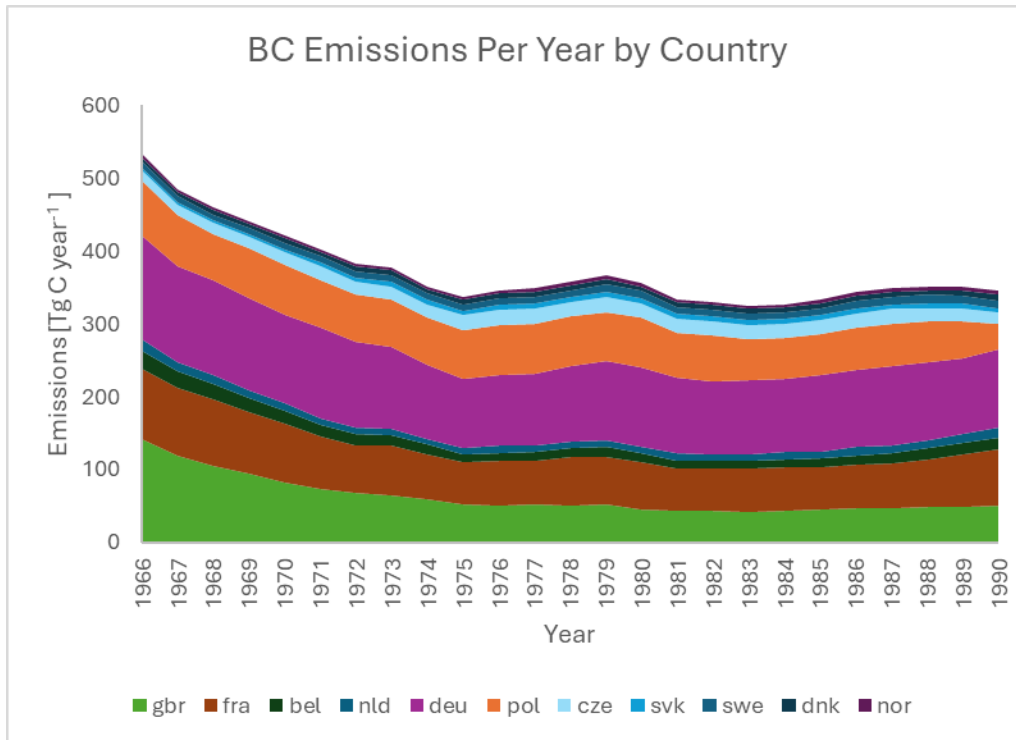


**Figure 3.24:** BC emissions by energy consumption (in Tg C year<sup>-1</sup>) per year by country (Hoesly et al., 2018).

Figure 4.14 is a good representation of BC emissions that were present in the European atmosphere from 1966 to 1990. The trends can be compared with aerosol concentration derived from Falsterbo's archive and socio-economic development of northern Europe can be studied in detail.

## 5. Conclusions

In conclusion, this research has demonstrated that archived filters from Falsterbo can be used to characterize daily changes in aerosol composition in the region. This was achieved through a combination of air mass back trajectory analysis and source apportionment analysis using HYSPLIT model, PMF and CWT technique.

Long-range air pollutants transported by air mass from Eastern and Southern Europe significantly impact the air quality in Falsterbo. The main sources of these air pollutants in 1972 were anthropogenic activities, including industrial activities, coal combustion, oil combustion, biomass burning, wood burning, dust and marine aerosols. Although many elements were detected in every filter of 1972, lead (Pb) and arsenic (As) were absent in a few filters. This absence explains that Sweden's ban on leaded gasoline was in effect, but no such bans were ratified in Eastern and Southern European countries in that time, leading to detection of the emission in Southern Sweden. Regulation of air pollution in one country is not sufficient to mitigate air pollution issues. While national legislation of a country can improve the quality of air, long-range transported pollutants from other countries continue to be a challenge.

Future research could focus on detailed daily aerosol concentration changes and their origin of emission from 1966 to 1990. Analyzing these changes as a function of time with powerful tools such as PMF and HYSPLIT model can provide deeper understanding into how socio-economic development have influenced to the air quality of Sweden. These approaches can provide with more interesting studies upon anthropogenic activities and the impact on air quality.

## ACKNOWLEDGEMENT

I would like to express my deepest gratitude to Jan Pettersson for his invaluable supervision and guidance throughout this project. His expertise and dedication have been instrumental in developing my skills as a researcher. I am also sincerely thankful to Johan Boman for his assistance with the EDXRF analysis and for patiently teaching me how to use the apparatus, including Xiangrui Kong, for guiding me with writing this thesis. His support and knowledge were crucial for the success of this project. A special thanks to Karin Söderlund, head of the Atmospheric Division at IVL Swedish Environmental Research Institute, for generously providing the filters from Falsterbo. Her contribution was essential to the progress of my thesis. Additionally, I am profoundly grateful to my colleagues for their unwavering support and encouragement throughout this project. Their support and encouragement have been greatly appreciated. Lastly, I am grateful to the University of Gothenburg for providing me with this opportunity and platform to conduct my thesis and gain experience that I can use in my future endeavors.

## 6. References

- Anderson, H. R. (2009). Air pollution and mortality: A history. *Atmospheric Environment*, 43(1), 142-152. <https://doi.org/10.1016/j.atmosenv.2008.09.026>
- Baker, J. (2010). A cluster analysis of long range air transport pathways and associated pollutant concentrations within the UK. *Atmospheric Environment*, 44(4), 563-571. <https://doi.org/10.1016/j.atmosenv.2009.10.030>
- Barregard, L., Sällsten, G., Gustafson, P., Andersson, L., Johansson, L., Basu, S., & Stigendal, L. (2006). Experimental Exposure to Wood-Smoke Particles in Healthy Humans: Effects on Markers of Inflammation, Coagulation, and Lipid Peroxidation. *Inhalation Toxicology*, 18(11), 845-853. <https://doi.org/10.1080/08958370600685798>
- Bergbäck, B., Anderberg, S., & Lohm, U. (1992). Lead load: historical pattern of lead use in Sweden. *AMBIO A Journal of the Human Environment*, 21, 159-165.
- Brimblecombe, P. (1987). *The Big Smoke: A History of Air Pollution in London Since Medieval Times*. Routledge. <https://books.google.com/books?id=bx4wAFE8xGUC>
- Brimblecombe, P. (1999). 2 - Air Pollution and Health History. In S. T. Holgate, J. M. Samet, H. S. Koren, & R. L. Maynard (Eds.), *Air Pollution and Health* (pp. 5-18). Academic Press. <https://doi.org/10.1016/B978-012352335-8/50077-6>
- Brimblecombe, P. (2006). The clean air act after 50 years. *Weather*, 61(11), 311-314.
- Brosset, C., & Åkerström, Å. (1972). Long distance transport of air pollutants—Measurements of black air-borne particulate matter (soot) and particle-borne sulphur in Sweden during the period of September–December 1969. *Atmospheric Environment (1967)*, 6(9), 661-673. [https://doi.org/10.1016/0004-6981\(72\)90024-8](https://doi.org/10.1016/0004-6981(72)90024-8)
- Calvo, A. I., Alves, C., Castro, A., Pont, V., Vicente, A. M., & Fraile, R. (2013). Research on aerosol sources and chemical composition: Past, current and emerging issues. *Atmospheric Research*, 120-121, 1-28. <https://doi.org/10.1016/j.atmosres.2012.09.021>
- Cohen, A. J., Brauer, M., Burnett, R., Anderson, H. R., Frostad, J., Estep, K., Balakrishnan, K., Brunekreef, B., Dandona, L., & Dandona, R. (2017). Estimates and 25-year trends of the global burden of disease attributable to ambient air pollution: an analysis of data from the Global Burden of Diseases Study 2015. *The lancet*, 389(10082), 1907-1918.

- Draxler, R., & Hess, G. (1998). An overview of the HYSPLIT\_4 modeling system for trajectories, dispersion, and deposition. *Australian Meteorological Magazine*, 47, 295-308.
- Fenger, J. (2009). Air pollution in the last 50 years – From local to global. *Atmospheric Environment*, 43(1), 13-22. <https://doi.org/10.1016/j.atmosenv.2008.09.061>
- Fleming, Z. L., Monks, P. S., & Manning, A. J. (2012). Review: Untangling the influence of air-mass history in interpreting observed atmospheric composition. *Atmospheric Research*, 104-105, 1-39. <https://doi.org/10.1016/j.atmosres.2011.09.009>
- Galloway, J. N., Thornton, J. D., Norton, S. A., Volchok, H. L., & McLean, R. A. N. (1982). Trace metals in atmospheric deposition: A review and assessment. *Atmospheric Environment (1967)*, 16(7), 1677-1700. [https://doi.org/10.1016/0004-6981\(82\)90262-1](https://doi.org/10.1016/0004-6981(82)90262-1)
- Grandjean, P., & Nielsen, T. (1979, 1979//). Organolead compounds: Environmental health aspects. Residue Reviews, New York, NY.
- Guerreiro, C. B. B., Foltescu, V., & de Leeuw, F. (2014). Air quality status and trends in Europe. *Atmospheric Environment*, 98, 376-384. <https://doi.org/10.1016/j.atmosenv.2014.09.017>
- Harmens, H., Buse, A., Büker, P., Norris, D., Mills, G., Williams, B., Reynolds, B., Ashenden, T. W., Rühling, Å., & Steinnes, E. (2004). Heavy metal concentrations in European mosses: 2000/2001 survey. *Journal of Atmospheric Chemistry*, 49, 425-436.
- Hoesly, R. M., Smith, S. J., Feng, L., Klimont, Z., Janssens-Maenhout, G., Pitkanen, T., Seibert, J. J., Vu, L., Andres, R. J., & Bolt, R. M. (2018). Historical (1750–2014) anthropogenic emissions of reactive gases and aerosols from the Community Emissions Data System (CEDS). *Geoscientific Model Development*, 11(1), 369-408.
- Hovmand, M. F., & Kystol, J. (2013). Atmospheric element deposition in southern Scandinavia. *Atmospheric Environment*, 77, 482-489. <https://doi.org/10.1016/j.atmosenv.2013.03.008>
- Hsu, Y.-K., Holsen, T. M., & Hopke, P. K. (2003). Comparison of hybrid receptor models to locate PCB sources in Chicago. *Atmospheric Environment*, 37(4), 545-562. [https://doi.org/10.1016/S1352-2310\(02\)00886-5](https://doi.org/10.1016/S1352-2310(02)00886-5)
- Johnsen, I., & Rasmussen, L. (1977). Retrospective study (1944-1976) of heavy metals in the epiphyte *Pterogonium gracile* collected from one phorophyte. *Bryologist*, 625-629.
- Kaijser, A., & Högselius, P. (2019). Under the Damocles Sword: Managing Swedish energy dependence in the twentieth century. *Energy Policy*, 126, 157-164. <https://doi.org/10.1016/j.enpol.2018.11.023>

- Karaca, F., & Camci, F. (2010). Distant source contributions to PM10 profile evaluated by SOM based cluster analysis of air mass trajectory sets. *Atmospheric Environment*, 44(7), 892-899. <https://doi.org/10.1016/j.atmosenv.2009.12.006>
- Koolen, C. D., & Rothenberg, G. (2019). Air pollution in Europe. *ChemSusChem*, 12(1), 164-172.
- Kovacevik, B., Wagner, A., Boman, J., Laursen, J., & Pettersson, J. (2011). Elemental composition of fine particulate matter (PM2.5) in Skopje, FYR of Macedonia. *X-Ray Spectrometry*, 40, 280-288. <https://doi.org/10.1002/xrs.1337>
- Kunc, J., Tonev, P., Martinat, S., Frantál, B., Klusáček, P., Dvořák, Z., Chaloupková, M., Janurova, M., Krajickova, A., & Silhan, Z. (2018). Industrial legacy towards brownfields: Historical and current specifics, territorial differences (Czech Republic). *Geographia Cassoviensis*, 12, 76-91.
- Markou, M. T., & Kassomenos, P. (2010). Cluster analysis of five years of back trajectories arriving in Athens, Greece. *Atmospheric Research*, 98(2), 438-457. <https://doi.org/10.1016/j.atmosres.2010.08.006>
- Murray, F. (2013). The changing winds of atmospheric environment policy. *Environmental Science & Policy*, 29, 115-123. <https://doi.org/10.1016/j.envsci.2013.02.005>
- Nielsen, H. (2017). Coal, commerce and communism: Empirical studies on energy history in the Czech Republic.
- Nriagu, J. O. (1990). The rise and fall of leaded gasoline. *Science of The Total Environment*, 92, 13-28. [https://doi.org/10.1016/0048-9697\(90\)90318-O](https://doi.org/10.1016/0048-9697(90)90318-O)
- Olstrup, H., Forsberg, B., Orru, H., Spanne, M., Nguyen, H., Molnár, P., & Johansson, C. (2018). Trends in air pollutants and health impacts in three Swedish cities over the past three decades. *Atmos. Chem. Phys.*, 18(21), 15705-15723. <https://doi.org/10.5194/acp-18-15705-2018>
- Pekney, N. J., Davidson, C. I., Zhou, L., & Hopke, P. K. (2006). Application of PSCF and CPF to PMF-Modeled Sources of PM2.5 in Pittsburgh. *Aerosol Science and Technology*, 40(10), 952-961. <https://doi.org/10.1080/02786820500543324>
- Pope, C. A., Thun, M. J., Namboodiri, M. M., Dockery, D. W., Evans, J. S., Speizer, F. E., & Heath, C. W. (1995). Particulate air pollution as a predictor of mortality in a prospective study of US adults. *American journal of respiratory and critical care medicine*, 151(3), 669-674.

- Schmalensee, R., & Stavins, R. N. (2019). Policy Evolution under the Clean Air Act. *Journal of Economic Perspectives*, 33(4), 27-50. <https://doi.org/10.1257/jep.33.4.27>
- Seibert, P., Kromp-Kolb, H., Baltensperger, U., Jost, D., & Schwikowski, M. (1994). Trajectory analysis of high-alpine air pollution data. *Air pollution modeling and its application X*, 595-596.
- Sörme, L., Bergbäck, B., & Lohm, U. (2001). Goods in the Anthroposphere as a Metal Emission Source A Case Study of Stockholm, Sweden. *Water, Air and Soil Pollution: Focus*, 1(3), 213-227. <https://doi.org/10.1023/A:1017516523915>
- Sreekanth, V., Tonne, C., Salmon, M., Arulselvan, S., & Marshall, J. D. (2019). The role of blank filter mass in attenuation measurements using an off-line transmissometer. *Journal of Aerosol Science*, 131, 41-47.
- Stein, A. F., Draxler, R. R., Rolph, G. D., Stunder, B. J. B., Cohen, M. D., & Ngan, F. (2015). NOAA's HYSPLIT Atmospheric Transport and Dispersion Modeling System. *Bulletin of the American Meteorological Society*, 96(12), 2059-2077. <https://doi.org/10.1175/BAMS-D-14-00110.1>
- Stunder, B. J. B. (1996). An Assessment of the Quality of Forecast Trajectories. *Journal of Applied Meteorology and Climatology*, 35(8), 1319-1331. [https://doi.org/10.1175/1520-0450\(1996\)035<1319:AAOTQO>2.0.CO;2](https://doi.org/10.1175/1520-0450(1996)035<1319:AAOTQO>2.0.CO;2)
- Wang, X., Jing, H., Dhungel, B., Wang, W.-N., Kumfer, B. M., Axelbaum, R. L., & Biswas, P. (2016). Characterization of organic and black carbon aerosol formation during coal combustion: An experimental study in a 1MW pilot scale coal combustor. *Fuel*, 180, 653-658. <https://doi.org/10.1016/j.fuel.2016.04.057>
- WHO. (1979). *Sulfur oxides and suspended particulate matter*. World Health Organization.
- WHO. (2006). *Air quality guidelines: global update 2005: particulate matter, ozone, nitrogen dioxide, and sulfur dioxide*. World Health Organization.
- Wichmann, H., Mueller, W., Allhoff, P., Beckmann, M., Bocter, N., Csicsaky, M., Jung, M., Molik, B., & Schoeneberg, G. (1989). Health effects during a smog episode in West Germany in 1985. *Environmental health perspectives*, 79, 89-99.
- Yang, Y., Lou, S., Wang, H., Wang, P., & Liao, H. (2020). Trends and source apportionment of aerosols in Europe during 1980–2018. *Atmos. Chem. Phys.*, 20(4), 2579-2590. <https://doi.org/10.5194/acp-20-2579-2020>

Zhang, Z., Wang, J., Kwong, J. C., Burnett, R. T., van Donkelaar, A., Hystad, P., Martin, R. V., Bai, L., McLaughlin, J., & Chen, H. (2021). Long-term exposure to air pollution and mortality in a prospective cohort: The Ontario Health Study. *Environment International*, *154*, 106570. <https://doi.org/10.1016/j.envint.2021.106570>